Experimental Investigation to Explore the Effects of Chromium and RE addition on Mechanical Behavior of Hardfacing on Grey C.I.

A Dissertation Submitted

in partial fulfilment of requirements

for the degree of

Master of Engineering

in

Production Engineering

by

Mohit Kanyathia

Registration No.: 801685013

Under the Supervision of

Dr. R.S. Joshi (Supervisor)

(Assistant Professor, MED)

Dr. V.K. Singla (Supervisor)

(Associate Professor, MED)

MECHANICAL ENGINEERING DEPARTMENT
TIET, PATIALA

JULY, 2018

CERTIFICATE

I hereby declare that this thesis report entitled "**Experimental investigation to explore the effects of chromium and RE addition on mechanical behavior of hardfacing on Grey C.I.**" is an authentic record of my work carried out as requirements for the award of the degree of **Master of Engineering** in **Production Engineering** at **Thapar Institute of Engineering & Technology, Patiala** under the supervision of **Dr. R. S. Joshi** (Assistant Professor, MED) and **Dr. V.K. Singla** (Associate Professor). No part of the matter embodied in this report has been submitted to any other university or institute for the award of any degree.

Mohit

Date: 31/07/2018

Mohit Kanyathia

801685013

TIET, Patiala

It is certified that the above statement made by the student is correct to the best of our knowledge and belief.

31/7/18

31/7/2018

Dr. R. S. Joshi
Assistant Professor, MED
TIET, Patiala – 147004

Dr. V.K. Singla
Associate Professor, MED
TIET, Patiala – 147004

Dedicated to

My Parents

Acknowledgement

I would like to express my deep gratitude towards my supervisors, Dr. R.S. Joshi and Dr. Vinod Kumar Singla, Department of Mechanical Engineering, Thapar Institute of Engineering and Technology, Patiala for their valuable guidance and support. Working under their guidance has been fruitful and worthful in the context of knowledge. I also like to thank Dr Sukwinder Panesar, Assistant Manager and Head, Alpha Test House at Mohali and all the other staff members as well for providing facilities for experimentation. I would also like to thank all the lab attendants at Thapar Institute of Engineering and Technology, Patiala for their valuable support in carrying out experimentation on wear testing, Microhardness testing.

I am very thankful to my parents, friends and colleagues for their support in preparation of this thesis report.

Mohit Kanyathia

801685013

TIET, Patiala

Abstract

Due to rapid growth in the industrialization and also in the field of urbanization, demand for repairing the equipment's increased. The hardfacing technique for repairing and increasing the life of equipment was one of them in the top of the list. "Preventive hardfacing" is the utilization of hardfacing procedures to the generation of a fresh component. In the current investigation the effect of various rare earth oxide with the addition to chromium was done to calculate the wear and corrosion behavior of hardfacing on grey cast. By using electrode of TENALLOY 16-7016 having a hardness of 150 BHN. First five samples were prepared for EBSD and for microhardness tester with chromium weight percentage of 1.7 %, cerium oxide with weight percentage of 0.6% and lanthanum oxide of 0.4 % and at last filled them in the groove on grey cast iron sample. The lanthanum oxide showed the refined grain structure in EBSD testing and the sample of chromium and lanthanum oxide showed least mean grain size. Micro-hardness testing done at dwell time of 20 seconds and at a load of 500 gm which showed maximum value of hardness which proved Hall Petch equation that the hardness component with least grain size showed the maximum hardness value. Pin-on-disc machine used EN 31 high speed steel and for this experiment six samples were prepared which were operated at 955, 764, 1273,546, 477and 637 rpm and after every 5 minutes the sample was weighted. From the calculated results it was observed that the chromium sample got less wear than the other samples and the maximum wear found in chromium and cerium oxide sample. For corrosion testing, salt spray chamber for 120 hours i.e. almost for 5 days placed under the spraying of Nacl solution. Results states that chromium and cerium oxide sample showed less corroded area among the other samples with area corroded of 18%. It can be inferred from the experimentation that the chromium and lanthanum oxide sample increased the hardness along with least abrasive size. During corrosion analysis the best sample was the chromium and cerium oxide with weight of 1.57% and in wear analysis the best sample to resist weight loss was the chromium sample with weight of 1.78%.

Contents

List of Figures

List of Tables

Nomenclature

HCCI	High Chromium Cast Iron
CeO_2	Cerium Oxide
La_2O_3	Lanthanum Oxide
mpy	Miles per year
HVN	Vicker's hardness number
$Fecl_3$	Iron chloride
Ethanol + HNO_3	Nital
Ethanol + Picric acid	Picric acid
ASTM-A36	Standard steel type
ASTM-B-117-11	Standard for salt spray chamber
EBSD	Electron backscattered diffraction
Ni-Cr-B	Nickel-chromium-boron alloy
mol/l	Molar Concentraion
g/lt	Grams per litre
EN 31steel	Emergency number 31steel
Mo	Molybdenum
Mn	Manganese
PTA	Plasma transferred arc welding
TiC	Titanium carbide

Chapter 1

Introduction

1.1 Hardfacing

During 1921, Brothers Shelly M Stoody and Winston E. started up stoody welding Co. for repairing growing farm implement and repairing of tractors equipment's. After couple of year they were started repairing drill bits and oil rigs.The stoody brothers were induced that there could be more idea to repair drill bits with having more durability and also remains sharper for longer time. They developed process of hardfacing and which can be remains in industry for many decades. Hardfacing technology was first taken place in the stoody laboratory. Hardfacing also called Hard surfacing which defined as depositing of alloy material on metallic part with the help of welding processes to acquire/achieve more desired corrosion & wear properties. The main purpose of hardfacing is to provide resistance to wear, corrosion. The hardfacing can also be apply to the newly made equipment and also revive the worn surfaces. This technique is used in every kind of manufacturing industries.

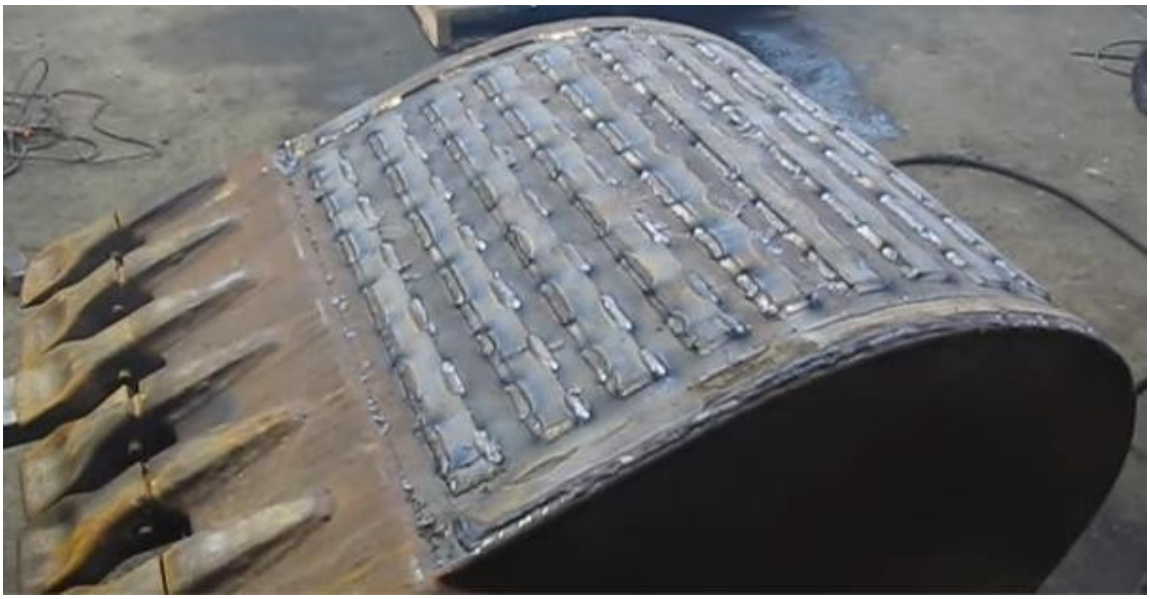

Fig. 1.1 Hardfacing (Courtesy quehanchongmon.com)

1.2 Hardfacing benefits

Most of companies utilizes hardfaced product due to the following reasons:-

1. It reduces cost of part which was installed that is about 25-75 % of cost of replacement part.
2. Increases the life of equipment from 30-300 times but also depend upon what kind of product is used for what application.
3. Also reduces downtime as part are last longer so less shut down required to change the part.
4. Minimizes inventory of spare parts. As worn parts can be rebuilt quickly so need not to store more spare parts.

1.3 Hard surfacing uses

1.3.1 The two major region at which hardfacing was done are

Recovery of worn samples There is no proper answer to stop the complete wear of the components. So the position must be received when all the equipment which are subjected to abrasive wear will arrive the ceiling of the advantageous life. The engineer has only two common ways either to repair or to replace the component. But during replacing of the component, cost to be paid for equipment was much higher than and also this effects to the inventory cost and sometimes engineer has to face downtime of the equipment.

The protection of new metal parts against the loss of metal Best about the hard surfacing was that, it was applicable to the old or used as well as the newly made component which was going to be affected by the wear. More the overlay of the alloy more will be the wear resistance and increase in the life span of the equipment with two or three times more than the wear effected component. Although the addition of any alloy was costlier but lesser than the price of the new component.

1.4 Selecting the suitable hardfacing process

The following things are to be noticed while selecting or choosing the hardfacing process. Hardfacing can be connected by various welding forms. As a rule, the hardware is indistinguishable or like that utilized for auxiliary welding. Determination of the most reasonable welding process for a given occupation will rely upon various variables including:

Function of part This states that about what kind of the part is requires as hardfacing is done on very limited components.

Substrate Metal composition Diverse procedures may have distinctive warmth inputs which render them inadmissible for certain base metal composes, e.g. manganese steels require low warmth info thus gas hardfacing would not be reasonable.

Size & Structure The Size and shape is the major fact that effects the type of Harding. Different welding were used as per the applicable to the component. The Irregular shape cannot be hardfaced easily and sometime requires only the replacement of the old component.

Accessibility It may not generally be conceivable to control overwhelming programmed gear into zones where work must be finished. Additionally, out-of position welding will restrict the selection of procedures.

Condition of repair Substantial severely worn segment require overwhelming reconstructing would be most appropriate to forms with high statement rates.

Number Depending upon the number of samples to be hardfaced and according to that the automatic or manual process was applied. For a smaller number manual hardfacing was done and for a large number automatic hardfacing was done as we know the cost of automatic hardfacing process more.

1.5 Dilution

Control of weakening is fundamental when surfacing. Weakening influences the synthetic creation of the store, hardness and quality. Amid welding, a portion of the base metal breaks up into the weld pool, weakening it.

Formula for dilution = % Dilution = B/A+B x 100

Fig. 1.2 diagram for deposit and dilution

1.5.1 Dilution is controlled by

1. Using the appropriate welding technique, especially heat input.

2. A cover between weld goes, of around half, gives great weakening control. Multi-pass surfacing brings about lower weakening than single-pass surfacing

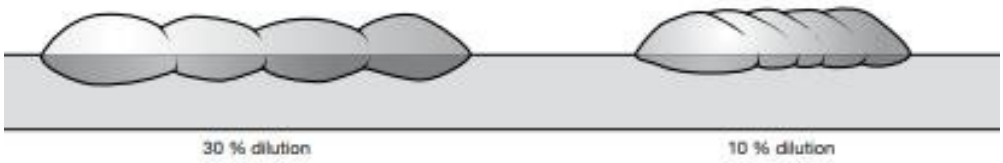

Fig. 1.3 Shows left side the dilution of 30 % and on the right side it shows dilution of 10 %. (Courtesy www.welding-alloy.com)

3. Selecting the usable polarity of current may be DC- , DC+ or AC. Which may effect rate of dilution.
4. The heat input depend upon welding process which can be the straight or inter-wined welding process.

1.6 Bead Pattern

At times, geometric weld dots give preferable wear opposition over a smooth hardfaced surface. This kind of store is a practical answer for wear caused by low or direct scraped spot, under low effect. For these applications, the kind of geometry to utilize depends straightforwardly on the size and properties of the grating.

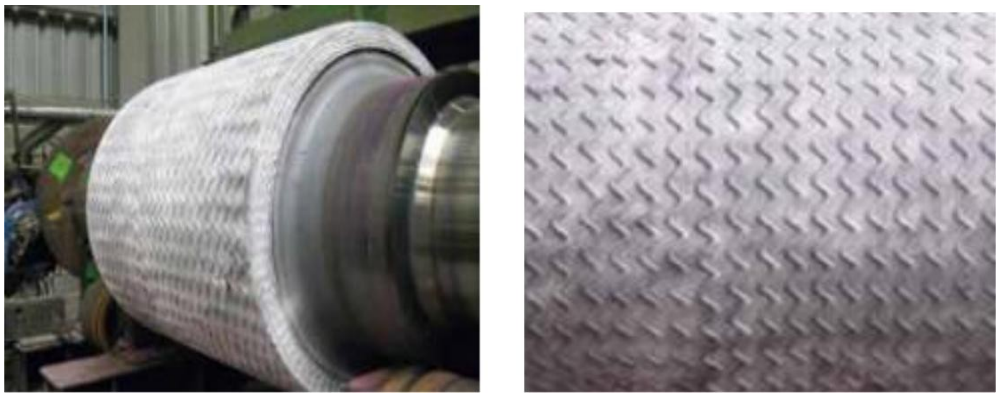

Fig1.4 Bead pattern with different side (Courtesy www.welding-alloys.com)

The standard of this kind of surfacing comprises of limiting relative development of the rough materials on the parts and making a hostile to wear obstruction by catching the material in the empty regions. The Fig. 1.4 represents the bead with two different angles which prevent the component from wear.

1.6.1 Types of pattern

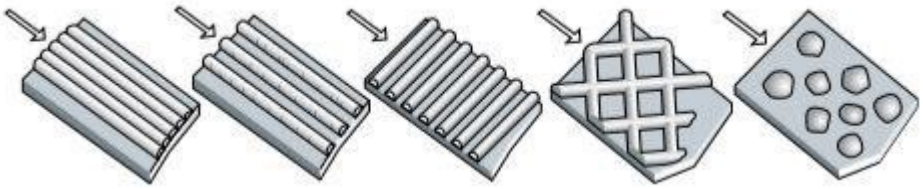

Fig. 1.5 (a) Continuous overlap (b) Regular interval (c) Grid passes (d) Spot welds (Courtesy www.afrox.com)

(a) Juxtaposed Passes to counter extreme scraped spot, the hardfacing is nonstop over the entire of the surface concerned. This guarantees there is no contact between the outside component and the base metal. The dabs are compared with a half interposes cover to ensure ideal surfacing attributes (by confining weakening). As a rule, the weld dabs are arranged in an indistinguishable course from the stream, along these lines permitting persistent entry of material

(b) Regular Intervals If there should arise an occurrence of low or direct scraped spot (without affect), surfacing might be constrained to isolated parallel dots. Separating of the dabs is a key factor that depends straight forwardly on the span of the grating. If there should be an occurrence of high scraped spot, the space between the dabs is decreased.

(c) Grid Passes Cross type of beads going to make grid like structure. Angle between the beads can be changed from 30^{0} to 90^{0}. This type of grid patterns can be applicable to less or more abrasive regions. The bead provide more abrasion in the interstices. The littler the non-surfaced zone, the more prominent the security given to the scraped spot surfaces by the fine particles.

(d) Spot Welds This kind of spot welds applied in a region where the wear was moderate. Mostly these kind of spots were formed on manganese steels because steel was badly effected by heat generated during the welding. The abrasive size tells about the space needed between the welding spots. Good abrasive provides less space between the spots. The better the grating, the littler the separation between spots.

1.7 Types of welding used for hardfacing

Shielded metal arc welding One of the most common and cheapest type of welding and also known as manual arc welding. Invented in 1888 by Nikolay, a Russian scientist. Both with AC or

DC current is used to perform the operation by the help of electrode sticks which are made up of different material composition as per used for the application. As the terminal melts, the transition covering deteriorates, radiating protecting gases that shield the weld zone from oxygen and other barometrical gases. Moreover, the transition gives liquid slag which covers the filler metal as it flies out from the terminal to the weld pool. When part of the weld pool, the slag buoys to the surface and shields the weld from sullying as it cements. Once solidified, it must be worn down to uncover the completed weld.

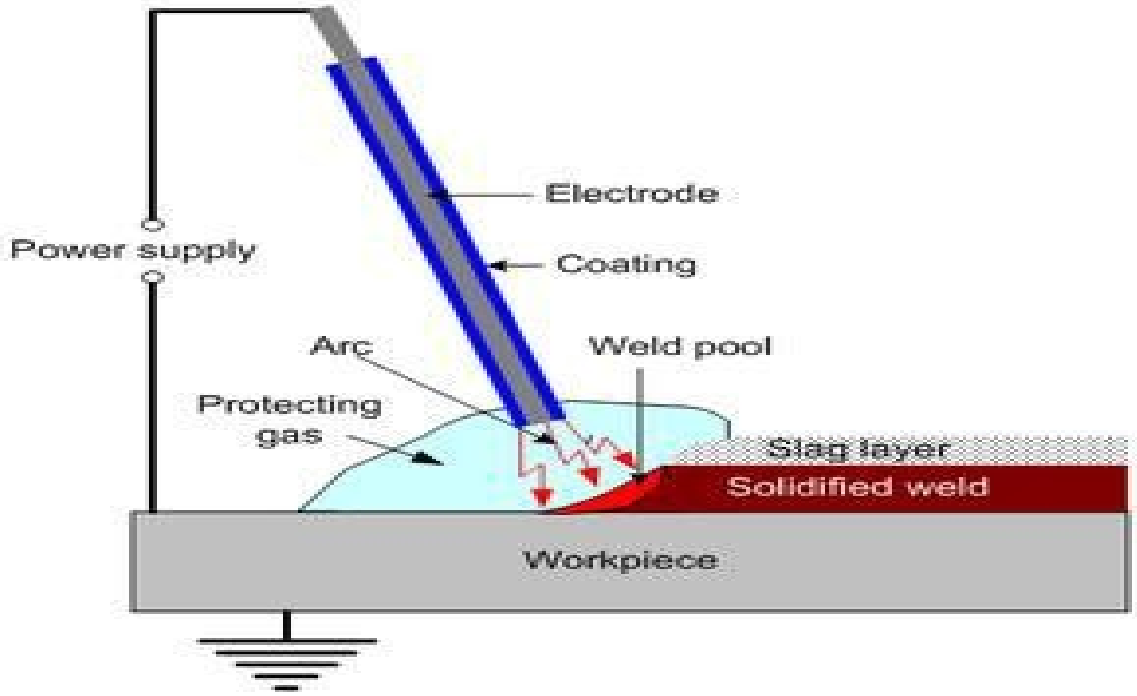

Fig. 1.6 SMAW type (Courtesy www.subtech.com)

Advantages

1. Cheapest method of the welding process.
2. Versatility which helps to weld distinct metals or the alloys without any interruption.
3. Also applicable to the outdoor applications.
4. No extra gas is required for the welding.
5. Hardfacing can be done by this kind of welding.
6. Easily available in the market.

Disadvantages:

1. Not applicable for long joints of welding.
2. The procedure is spasmodic because of restricted length of the electrodes.
5. To change the electrode, quick start and stop is needed.
6. Butts of the electrode are of no use.
7. Sometimes large amount of slag is formed.
8. Skilled worker is needed to operate with sound weld.
9. Presence of fumes gives difficult phase to operate the process.

Flux core arc welding

Flux cored arc welding: This was invented in 1950 by Bernard. It is a procedure that is firmly identified with Metal Inert Gas Welding. The two procedures utilize comparable gear and persistent wire bolsters, and both MIGW and FCAW utilize a similar kind of intensity supply. Motion Cored Arc Welding regularly utilizes a protecting gas like the MIGW procedure. Be that as it may, Flux-Cored Arc Welding may likewise be performed without a protecting gas. Also, this sort of welding is a significantly more beneficial process than MIG welding. Truth be told, FCAW is the most gainful of the manual welding forms.

Transition Cored Arc Welding is an extremely adaptable welding technique. This sort of welding is reasonable for all position welding with the best possible filler metal and transition arrangement. The high affidavit rates of FCAW add to the efficiency of this procedure, which furnishes quality welds with astounding weld appearance. Usually utilized for welding thicker areas and can deliver a completely entered weld on the two sides of half-inch plate in a solitary pass. The materials that work best with Flux-Cored Arc Welding are carbon steel, treated steel, and low-amalgam steels. Lamentably, most non-ferrous metals, including aluminum, can't be welded utilizing the FCAW technique. In light of its high welding speed and the capacity to be performed outside, even in breezy conditions, Flux-Cored Arc Welding is much of the time utilized as a part of the development business. As Fig. 1.7 clearly mentioning about the labelled diagram of flux core welding.

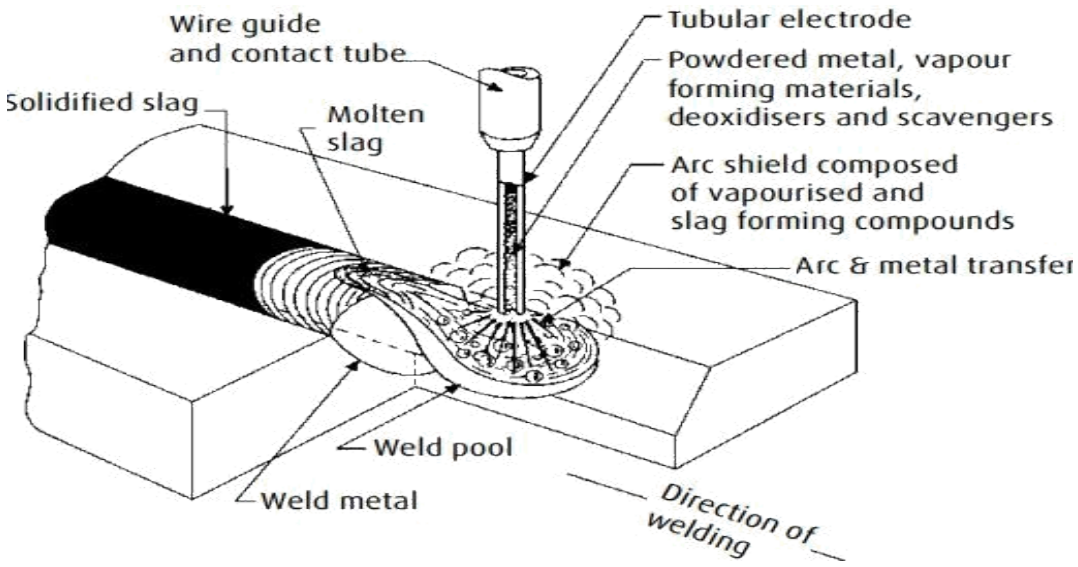

Fig. 1.7 Flux core welding (Courtesy www.weldingis.com)

Advantages of flux cored arc welding

1. Suitable for variety of alloys
2. Deposition value is more than SMAW up to 11 Kg/hr.
3. Both skilled and unskilled can operate this type of welding.
4. No initial cleaning of the metal is required.
5. Easy to operate without the use of shielded gas.

Disadvantages

1. For dilution a few layers are expected to get greatest wear properties.
2. Costlier than the SMAW type of welding.
3. Porosity is the common effect of this kind of welding.

Submerged arc welding: It was started at 1935 by Jones and Kennedy. Submerged curve welding (SAW) is so named in light of the fact that the weld and circular segment zone are submerged underneath a cover of transition. The motion material winds up conductive when it is liquid, making a way for the current to go between the anode and the work piece. The transition cover counteracts splash and starts, while protecting bright light and exhaust that are typically a piece of protected metal circular segment welding. The transition for the most part is provided to the welding head by means of a little container. An accumulation framework assembles the abundance

motion for reuse. The procedure utilizes at least one persistently sustained anodes (wires) to keep up a curve. SAW is known for its capacity to store a lot of metal rapidly, reliably, and securely. The fundamental SAW gear is a power source, control unit, wire unit, and spout. Motions utilized as a part of SAW are granular fusible minerals containing oxides of manganese, silicon, titanium, aluminum, calcium, zirconium, magnesium and different mixes, for example, calcium fluoride. The motion is uncommonly planned to be perfect with a given terminal wire write so the mix of transition and wire yields wanted mechanical properties. All motions respond with the weld pool to deliver the weld metal synthetic organization and mechanical properties. Usually practice to allude to motions as 'dynamic' on the off chance that they add manganese and silicon to the weld, the measure of manganese and silicon included is affected by the circular segment voltage and the welding current level.

The Process Variants are the wire and the flux. The wire used may be of twin or the triple. The flux has two type one is bonded and other is the fused fluxes.

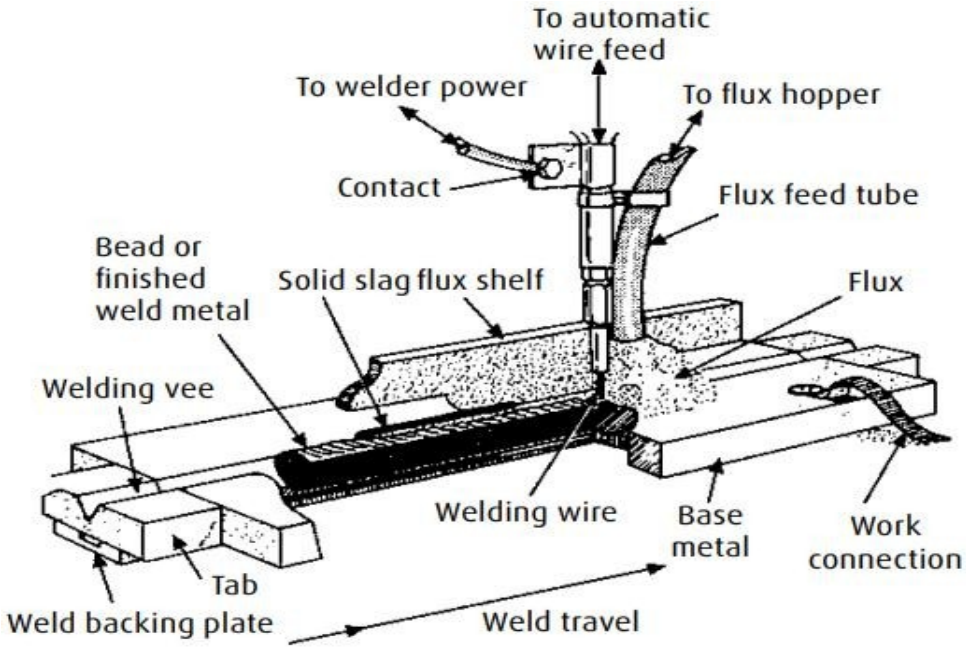

Fig. 1.8 Submerged arc welding (Courtesy Slideplayer.com)

Advantages of SAW

1. Due to high welding speed, distortion is less.
2. No spark or the smoke is found in this type of welding.

3. Also operated in the region of exposed areas and in the high speed winds.

Disadvantages

1. Porosity occurs due to the contamination.
2. Applicable to a limited variety of alloys, non-versatile.
3. Replacement of the flux is required and it is expensive.

Plasma transferred arc

Another important welding used for hardfacing. It works under the direct current current only and provides clear coating. Plasma-exchanged circular segment welding (PTA welding) is a warm procedure for applying wear and consumption safe layers on surfaces of metallic materials. The exceptionally fiery plasma circular segment liquefies the surface of the base material. In the meantime, the fine filler material is embedded into the bend and furthermore liquid. Amid cementing, a substance-to-substance bond between the filler material and the base material is made.

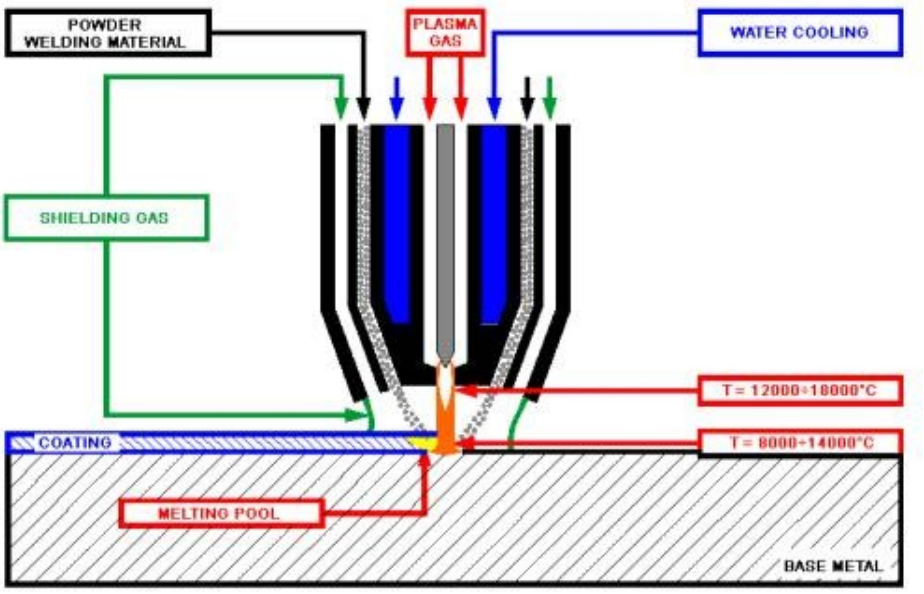

Fig. 1.9 Plasma transferred arc type (Courtesy www.commersald.com)

Advantages of PTA welding

1. No dilution of the deposit take place.

2. Also used for automation.
3. Easy to use and forms very smooth surface

Disadvantages

1. Difficult to move freely from one level to another.
2. Initial and maintenance cost is high.
3. Oxidation take place.

Powder spraying (flame spraying)

Powder welding brings about a smooth, thick covering with a dispersion attach to the base material. A standard oxy-acetylene burn is utilized, with the powder sustained into the fire from an appended hopper. The strategy is regularly utilized for glass molds, littler parts and repairs and is especially suited for the repair of cast press and machined parts, i.e. for working up edges and corners. Equipment utilized can be either hand held splashing lights or advanced metallizing guns for more specific applications

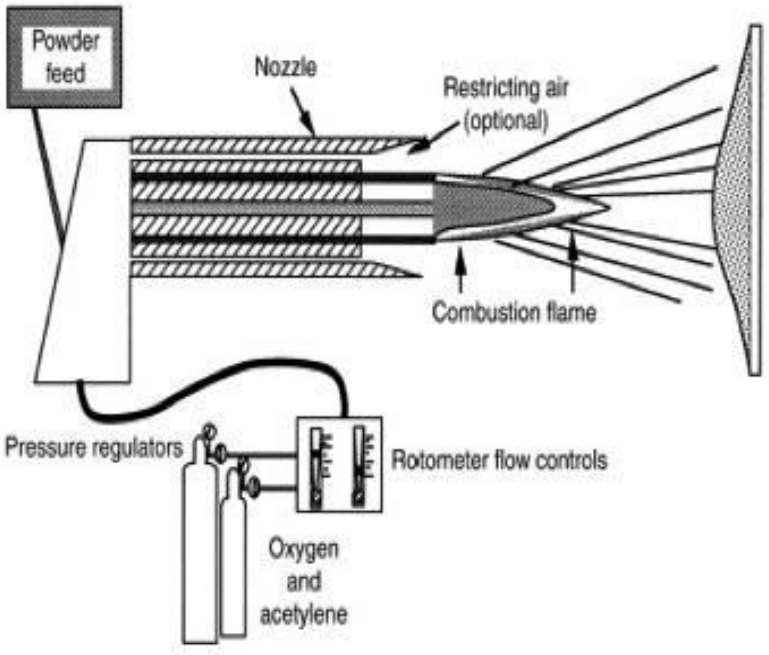

Fig. 1.10 Powder spraying (Courtesy weldguru.com)

Advantages of powder spray

1. No skilled worker required.
2. No dilution of the deposit take place.
3. Also used for automation

Disadvantages

1. Large amount of heat produced while coating.
2. High porosity take place around 10-25%.

1.8 Afrox

Afrox is African oxygen limited, which was started in 1927. It has 31 units in Africa and 16 units on the other countries worldwide. This company use to make large number of welding products and the gases.

Table 1.1 Some of the examples of hardfaced electrodes made from Afrox

S No.	Type	Applications	Hardness(HRc)
1.	Afrox 300	Track links, mine car wheels	26-31
2.	Afrox 350	Rail ends & rail lines	32-40
3.	Afrox 400	Tractor idlers, cable sheaves	37-47
4.	Afrox 452	Tractor drive sprockets, crane drive wheel	43-48
5.	Afrox 600	Earth scoops, conveyor screws	47-60
6.	Afrox 600A	Punches, chisels, axial, dies	53-58
7.	Afrox CrMn	Rail crossing, loader buckets	48-55
8.	Afrox NiMn	Swing hammer, dredger bucket	45-55
9.	Afrox CR70	Sugar mill roller, Excavator teeth & bucket	49-59
10.	Afrox CR70MR	Sugar mill for knives & hammers	49-59

Chapter 2

Literature Review

M.R. EL-Hebeary et al. [1] observed reduction in diameter of mill roller of sugar cane industry after every working period of time and these mill rollers had great significance in having beneficial effect in the production rate of sugar industry. Reduction in the diameter of roller is due to abrasion take place during crushing of large number of sugarcanes in the rollers. In this analysis, around sixty six samples of grey cast iron were carried for experimentation by using different elements like silicon, chromium and manganese with varying percentage. of these samples and performed the wear test at operating parameter such as load at 20N , speed at 1.28 m/s with disc diameter of 100mm, track radius of 0-40mm and the hardness of disc is 60HRC whereas the sample of cast bars with dimension of 50mm in diameter and length of 350mm was taken in testing. It was found that with addition of manganese by percentage of 0.58 to 3.00 there was increase in the hardness continuously but with increase in silicon from 2.99 to 3.00 %, hardness decreased and along with increase in chromium percentage from 0.520 to 2.11%, also seen that with chromium addition the graphite content decreased and that helps to resist abrasion as well as wear of the sample. From the 11 samples, the highest hardness was found to be from sample which had maximum silicon(2.11%),chromium(3.00%) and manganese(2.11%) content .in tensile test , manganese(3.00%) and silicon(2.02%) showed maximum ultimate tensile strength but as far the silicon amount increased from 2.59 to 3.00 %, there was drop in the value of tensile strength. XRD analysis of all samples failed to determine the types of carbide available in the samples after addition of different elements but showed the main phases like alpha Fe and Fe3C type. For the morphology of worn surfaces in SEM testing, it was found that with increase in content of manganese and chromium the damage to the surface is decreased but with the addition of silicon content the surface damage is increased. During SEM testing it was also observed that the volume of soft graphite flake decreased with the little gain in the manganese content and with the addition of chromium content there was increase in pearlite volume fraction which also elevates the hardness of the samples. In this paper, researchers observed best mill roller of grey cast iron had

composition of 3.04% C, 2.11% Si, and 2.11% Cr, P with 0.12% and S with 0.039% in it. Lowest value of wear rate was at 3.00% of Mn, 2.11% of Cr and Si was observed.

Giovanni Straffelini et al. [2] investigated the effect of heat treatment of disc on the wear and friction behavior. In their experimentation, authors employed disc made of low metallic friction material with composition of (Cu+Fe%=10-50%). Two disc were used from it in which one was untreated and second one was treated at 850 ^{0}C for 2 hours and then quenching for 1 hour at temperature of 180 ^{0}C. The untreated disc had micro hardness of 287±37 and treated one had 717±48. From the results it was found that heat treated disc showed high decrease in average friction coefficient and drop in contact temperature whereas highest value was given by untreated disc. As far as wear was concerned, the untreated disc had highest wear rate for pin (5.78mm^3/min) 10^{-7} and specific wear coefficient for pin (1.20 m^2/N) 10^{-14}. Experimentation explained that there was no co-relation between wear rate and surface finishing of the discs. The value of steady state friction coefficient for untreated disc was 0.5 but the treated disc after grinding was 0.4. After every change in pin on temperature took place, the temperature rise was in heated disc was lower than that of untreated disc and the highest temperature rise was observed in heated and ground disc.

V.E. Bundanan et al. [3] investigated the effect of two distinct hard-faced electrodes deposited on grey cast iron. Several tests were performed to study the microstructure of sample such as optical microscopy and SEM (scanning electron microscope) technique. In this paper, both electrodes had distinct composition. The carbon content was calculated to know that the sample is hypereutectic, eutectic, hypoeutectic. The value of carbon content was less 4.3% represents the sample was hypoeutectic and if more than 4.3% it would hypereutectic. In this experiment one electrode was hypoeutectic and second one was hypereutectic. By testing samples in XRD, it was found that first electrode coating showed large austenite, M_7C_3 and ferrite whereas second coating showed M_3C_2 and M_3C types of carbides. The SEM testing revealed that microstructure of first upper layer of first electrode was found to have M_7C_3 carbide in austenite matrix. The carbide present in the first sample coating was of rod like shape. The second coating on sample represented the cellular structure along with skeleton of types of carbides in austenite and the ferrite matrix. I was also found that first electrode coating showed larger volume fraction than second electrode and also had larger hardness shown by first one of 718(Vickers hardness) at distance from base

metal was 5mm and second electrode coating had showed 337(Vickers hardness). In wear weight loss by first electrode is less as compared to the second one. But the cane juice showed more weight loss in first than second electrode coating at load of 80N. As per results of SEM testing, it was observed that the first electrode coating showed good surface finish rather than second electrode. Under the BSE images taken from SEM, it was seen that first electrode had micro pitting whereas second had micro cracks only at the boundaries. It was also clear that hardness also dependent upon types and volume fractions. Results in slurry case is that the second electrode delivered lower wear rate and also good corrosion resistant than first electrode.

F. Fernandes et al. [4] elucidated the change in microstructure as well as the wear behavior of grey cast iron on using plasma transferred arc process by changing arc current. Nickel hard faced elements used to deposit the coating on grey cast iron. After deposition, different tests like SEM, XRD analysis, micro hardness took place to know the effect of the used nickel based elements, PTA process had performed better coating than other technique like flame spray and also had low porosity. To study the microstructure of the samples, first polishing and then etching was done by using etchants such as nitric acid with the addition of glacial acetic acid. So further for less brittle phases to be present during testing few of the samples were taken under heat treatment process. The microstructure of four distinct regions were seen first one of which was the weld portion which exhibited presence of graphite flake and precipitates. Second structure depicted heat effected zone showed the presence of martensite which was needle shaped. The dilution also dependent upon the current as per explained in this paper that with increase in current from 100-140 A the more dilution take place. SEM explained the presence of two phases of which one was light grey having silica rich elements and on other was chromium rich. Grain boundaries of the sample had the presence of the c flakes. PMZ that is partially melted zone had cementite which was white kind of phase. The maximum hardness values were shown in PMZ as compared to other zones which is of 538 (Vickers hardness). Conclusion revealed that with acceleration of arc current there will increase in c flakes as well as the precipitates in the especially the boundaries of the grain but on the other hand tremendous decrease in the hardness of the welded portion was seen.

XIAN faai et al. [5] experimented on impact of Mo (Molybednam) on the grey cast iron. Mo varied from 0.02 to 0.55 % for three different samples. All three samples were prepared by casting. The nital (4%) used as etchant to see the microstructure from optical microscope. The presence

precipitates were found with the help of J mat pro formula. M_2P type of phosphide present in all the samples which were considered in this research. The sample with least presence of Mo showed M_7C_3 carbides and with the increase in percentage of Mo, M_2C carbide shown along with some other carbide with very small fraction of $M_{22}C_6$. All the samples were seen firstly without etching such that the graphite flakes were showed by the samples whose length increases and then drop down depending upon the Mo expansion on to the samples. Mo expansion showed different images in BSE for all the three samples which contains Mo at different levels and Mo showed some of micro isolation and the precipitates during morphology in the place of micro segregation. The ultimate tensile strength showed increments immediately after reduction along with the increasing percentage of Mo. Mo addition increments the volume fraction of the precipitates. Mo is one of the best component that changes the mechanical properties of grey cast iron.

M. Pouranvari et al. [6] showed the nickel deposit effect on the grey cast iron using manual men arc welding. Vickers micro hardness test utilizing 200 g stack was done to acquire normal hardness of different microstructural zones in the weldment. In the wake of welding, a few examples were instantly exchanged to an electric heater, kept there at 870 C for 1 h and afterward heater cooled to the room temperature. In fusion zone, it comprised of fundamentally an austenitic network in addition to little measure of scattered graphite particles. In their experimental work, welding was done at 120 A current and at speed of 100 (mm/min) by using nickel electrode of 4m diameter. By using nickel based electrode various benefits were seen as nickel has obstruction to cracking in fusion zone also give better machinability. At PMZ the martensite was seen and this region has large number of carbides which after cooling the welding sample, it formed eutectic type carbide. At the boundaries austenite was found which at lower temperature seemed to be like martensite. The HAZ has austenite matrix along with availability of graphite flakes with higher volume fraction. Amid quick cooling rate regular of welding, HAZ microstructure changes to a weak structure. Since, the cooling rate is high, the graphitization process can't be expert. Additionally, the shaped austenite is changed into a hard fragile martensite because of the inborn high hardenability of this austenite. Two key methods of PMHT were tempering and annealing. The hardness of sample showed at different region in descending order such as PMZ ≥ HAZ ≥ FZ ≥ BM.

Chengyun et al. [7] explained about the TiC particles strengthened dim cast press composite manufactured by laser cladding of Ni– Ti– C framework on grey cast iron. Laser cladding was done on grey cast iron plate which is of rectangular shape and Co_2 laser used with diameter of beam was 4mm. Before testing of samples, etching was done by using distinct etchants such as hydrochloric acid nitric acid and sulfuric acid. At 14 % wt. of TiC dendritic structure showed in SEM testing. When wt. % was 20, blocky shape was shown. The hardness of the samples with 8, 14, 20 wt. % increases with addition of TiC and on other hand wear rate decreases as observed by the authors. The least wear rate was shown was at 20 % of TiC with value of 0.12 (mg/min). The surface unpleasantness additionally had incredible effect on wear rate.

D.G. McCartney et al. [8] explained the Fe-Cr-C coating on grey cat iron with the help of manual men arc welding and arc spraying. Microstructure of the samples were seen which showed M_7C_3 carbide in the austenite matrix of the shielded manual arc welding sample. These carbides are of rod like shape and the porosity found having volume of 3.2, 1.2, 6.5 at different samples. As per the author explained that micro hardness does not proportional to the mass loss. Now the turn come of the arc spray coating, in which wear test showed different modes includes micro cutting and plastic deformation. In some cases oxides were also found in some of the samples. At the end author concluded that arc spray can be used to overcome the difficulties found in SMAW and also provide more wear resistance as compared to manual welding

Xiaowen et al. [9] revealed the vanadium effect starting from 0% to 3% on high chromium cast iron. Along with the vanadium four more elements such as manganese (0.45%), silicon (0.15%) and chromium (25%) also provided in the flux. Talking about the micro hardness of the samples welded with wire which was cored with flux t load of 300 N. Six observations were took place for testing hardness. Types of carbides present in sample found by SEM, which showed welded region as hexagonal shape and some of these are like rod shape. 1784(Vickers hardness) of primary carbide showed the maximum value. Welded metal showed M_7C_3 carbide and in some regions austenite was also seen along with the martensite with the help of XRD analysis. With the addition of vanadium to the samples , it showed precipitation of different carbides were taken place and microstructure get refined which results in drop of dimensions of carbides. Vanadium addition also had significant impact on wear resistance as it reduces mass loss. From the Fe-C phase structure it was clear that with the use of vanadium from 0 % to 3 % the phase of primary carbide

reduces as we add vanadium whereas the eutectic carbides structure showed increment. Calculating by thermal – dynamic the temperature of VC precipitation it was shown by DSC curve that primary carbide showed temperature of 1327.2^0 C and other than that the eutectic carbide showed temperature of 1183.5^0 C. The wear rate of the samples decreases with the increment of additive (Vanadium).

Yinhu Qu et al. [10] determined the cause of cerium on high chromium cast iron having (chromium about 20 % and carbon about 4 % wt) on its structure by performing distinct testing techniques. Cerium added in composition of grey cast iron at four distinct level starting from 0 % to 1.50%. M_7C_3 type carbide seen during morphology also seen that as addition in cerium increases carbide size. The region with white in color represent in EDS spectrum the heterogeneous nucleus. The element S present in sample checked by EDS which showed the content less than 10%.Ce_2O_2S so called heterogeneous nuclei because it was observed that lattice misfits were less than 6 %. Lattice misfit was calculated and the fact for best result of nuclei was that the δ delta should be less than 6% , medium effect seen at 6 to 12% otherwise above 12% it will be least effective.

Xiaohui Zhi et al. [11] explained the hypereutectic HCCI microstructure by using niobium from 0.5% to 1.5%. Using nital of 5% to see the microstructure in optical microscopy, dimensions of sample was 60x60x20mm. Average diameter for carbide also solved. Isentropic like carbides M_7C_3 seen by increment the niobium. Major effect of niobium was seen after XRD analysis which revealed that with the addition on niobium, the carbides reduces in its number and along with this author reveled that volume fraction of the carbides also decreases.

Renzo Victoria et al. [12] explained the effect of sugarcane juice by performing different test techniques. Roller are made up of carbon steel (ASTM-A36). The wear test was started at load of 368.8 N and with sliding distance of 15000 m. In slurry condition, the wear rate was more rather than dry condition. No change in roll was seen with buffer of austenite and very minor change was seen during wear test. Corrosion occurred on steel without the silica grains. Highly variability was seen which was due to the roughness of the surfaces.

Minlin Zhong et al. [13] experimented on grey cast iron to know the effect of NiCr by laser cladding on the basis of corrosion as well as wear behavior of the samples. Ni with weightage of 75 % mixed with chromium of 25 %. After preparing the samples, corrosion testing took place by the use of H_2SO_4 and along with other solution of NaoH (Con. 0.5 mol/L). The base metal with

dimensions of 15mm x4.5mm x 2.8mm. The carbon dioxide laser used for the experiments and wear test was performed on block on ring. From EDS analysis it was clear that austenite containing nickel whereas the cementite containing chromium. Diluted NaOH solution and Diluted H_2SO_4 solution was used for corrosion testing to study the APC. The corrosion can be less only by having stable passive and secondly to control the thermodynamic stability by the use of alloying elements. Also the major change was seen by having a wear test with laser cladding samples.

D Womersley et al. [14] explained the results under the performing two different welding techniques for hardfacing on grey cast iron in which one technique includes thermal spraying on the other side to harden the face of grey cast iron , spraying of the powder was done. In thermal spraying (also known as metal spraying) Ni-Cr-B alloy used at temperature of 93^0 on the grey cast iron base metal, during spraying the temperature of the base metal temperature should be beneath 260^o.The fusion process the Ni-Cr-B deposit was converted to homogeneous covering and this process of fusion is one of the best technique which makes the substrate with least cracking effect. Deposition of the coating was varied from 0.5 to 2.15 mm. Now talking about the powder spraying, oxy-acetylene mixed with power and then deposited on substrate starting from right to left traverse. The thickness of the covering was 0.05 to 2.50 mm. A rectangular type of sample was prepared for testing. After performing the abrasive wear test at varying load and at average speed of 3.33 cm/sec. As results showed that double layered coating made less wear than single layer coating. But finally both the techniques of welding reduces wear about 3 to 50 %.Not such big difference was observed while performing with two different welding.

S. Chatterjee et al. [15] showed changes that can take place by making use of high chromium and carbon type electrode in welding on cast iron. Grey cast iron with grade of 2500 in ASTM of rectangular shape was used for performing testing. For wear testing the electrode baked for 2h at 100^0C and deposition take place with and without preheat and for preheat treatment the sample place in furnace at 400^0C. For metallography and hardness test the sample with dimensions of 20mm x 25mm x 12mm was used. The metallography test was took place after polishing the sample and etched by using the vieglla reagent and the microstructure was observed. Results on cracking it was clearly showed that cracking was more in double coating than single coating on other side the preheated showed less cracking as compared to no preheating done on the samples.

Hardness was seen when the sample was hardafaced without buffer layer. Preheat was played main significant in giving different results as on cracking and bond strength.

John J Coronado et al. [16] explained that what changes could took place after using different welding techniques for hardfacing on the substrate G65 of ASTM standard in its microstructure worn surface, hardness and its wear behavior. FCAW showed maximum hardness with value of 695 at a current of 250 A and heat input was 12.5 kj/cm and minimum hardness was seen with SMAW at current of 100 A and heat input of 7.1 kj/cm. During wear test the mass loss was observed at 3 layered sample of SMAW type with value of 4395 mg and least mass loss seen at FCAW type at 3 layered sample with value 779.33 mg. Martensite observed in single layer of FCAW type and some cracks also appeared in the matrix whereas austenite seen by using three layers coating by FCAW type in the eutectic matrix. EDS analysis showed types of carbides present and few of them are rich in titanium, chromium. Such molybdenum had significant role in incrementing the hardness of the sample and also provides the reduction in the wear rate. In SMAW, the presence of austenite seen in the eutectic matrix. Major difference was observed in single and 3 layers was the difference in the volume fraction of carbides. FCAW technique helpful in better abrasion resistance than SMAW due to presence of titanium content in the matrix.

Chieh Fan et al. [17] experienced the change in microstructure of steel by using hardfacing alloys which are rich in chromium by depositing them by using GTAW welding. A rectangular sample of 40mm x 40mm x 10mm was taken to deposit the cover of Cr-Fe-C alloy. Coating had thickness of 2-3mm and after the deposition alloy no cracks were observed. During XRD analysis $(FeCr)_{23}C_6$ carbide seen in which the structure formed was the fcc type structure. With the addition of some graphite to 5% the eutectic structure was appeared with the alpha structure of Fe-Cr matrix. The hardness comparatively decreases with graphite addition. The maximum hardness value recorded was 65 with carbon content of 3.357%. Chemical composition of all the four samples were recorded by using EPMA technique which results that carbon content with 2.99% showed hypereutectic structure and when carbon was at 0.357%, it showed eutectic structure(dendritic type) and hypereutectic had fine lamellar structure.

Xiaohui Zhi et al. [18] experimented the cerium on HCCI (High chromium cast iron) to study the change in its microstructure and some properties of HCCI having chromium up to 20%. Composition of high chromium cast iron had carbon of 4.17%, Chromium of 19.70%, Silicon of

1.16%, Magnesium of 0.80%, and Phosphorous of 0.04 %. Such that cerium was added in four samples with different weight proportion includes 0%, 0.5%, 1%, 1.5% respectively. Before studying the sample under optical microscope, the etchant which was nital of 5% was used for etching. The average diameter of the type of primary carbides was calculated at two different place and the position A resulted in small diameter as compared to position B which was may be due to chilling effect. It was also clear that structure get more refined with the addition of cerium. Through the TEM testing, the microstructure showed two phases of carbides one was the M_7C_3 carbides and other one was the Ce_2S_3 carbides in which M_7C_3 carbide had hexagonal lattice kind of structure and Ce_2S_3 carbide having fcc type of structure.

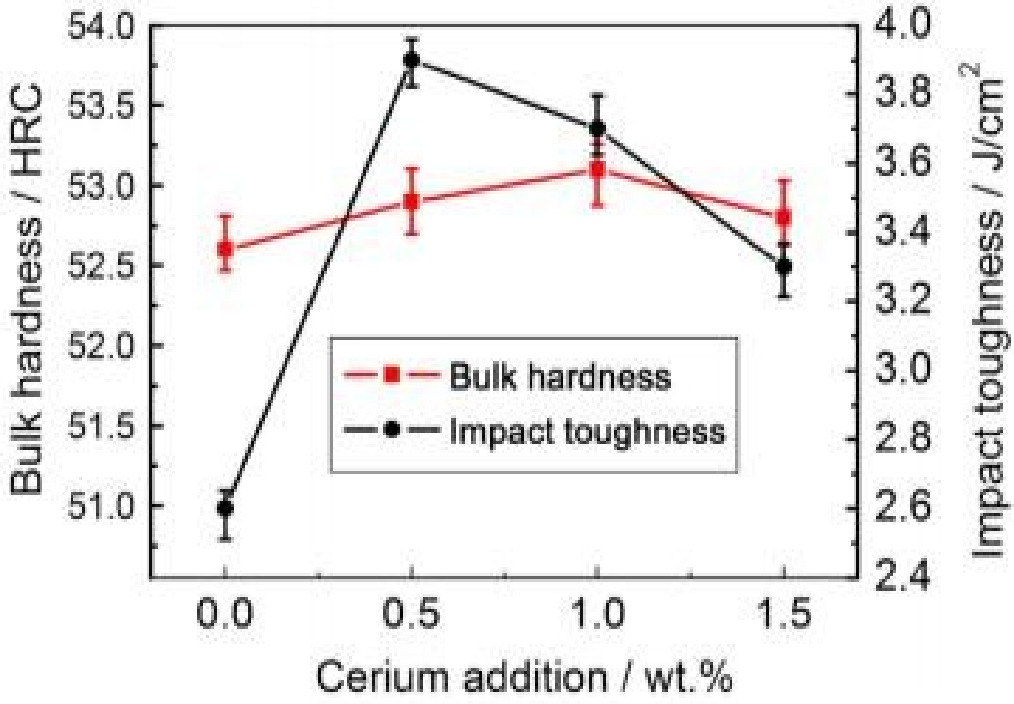

Fig.2.1 Showed the impact of cerium on hardness and toughness of cast iron

Very clearly it was shown that the cerium up to 0.5%, resulted in increase in toughness and decreases with the more than 0.5%. On the other side hardness increases from 0 to 1% and decreases with addition of cerium more than 1%.

XING Shule et al. [19] investigated the effect of cerium on Q235 steel with hardfaced alloys by varying the percentage of cerium in alloys by using flux cored welding. The chemical composition of the flux was mentioned in the table 2.1. Such that Fe-Cr13-Mn-Nb alloy was

used in which cerium was added in flux core wire. The rare earth oxide was very much commonly used to improve the wear properties. Some of the paper also mentioned that with cerium, the fracture toughness had great impact on the properties of wear resistance.

Table 2.1 Welding parameters

Welding Current/A	Welding voltage/V	Welding speed/(m/h)	Interpass temperatures/°C	Electric current electrode
280–350	23–27	14–18	<200	DCEP

Table 2.2 The chemical composition of flux was given below

Core powder	Content/wt.%
Fluorspar (CaF_2)	5–8
Oxides (TiO_2, ZrO_2, MgO, SiO_2)	18–23
Potash feldspar ($K_2O{\cdot}Al_2O_3{\cdot}6SiO_2$)	2–5
Alloying element	51–61
Deoxidizer (Si, Mn)	6–9
Ceria	
1# flux cored wire	0
2# flux cored wire	5
3# flux cored wire	10
Iron powder	Balance

Firstly talking about the SEM test, the two phases were present one was martensite and another one was the austenite in which the size of martensite showed decrement with the addition of cerium which makes refined structure. It was also clear that with the addition of cerium, the hardness of the sample increased and the due to addition of cerium, the grain were more refined which had large impact on toughness and due to this sample becomes less plastic deformed.

A. Wiengmoon et al. [20] explained the effect of chromium by varying its weight percentage from 20 to 36% in three different stages. But the first two alloys were go through heat treatment process. The samples were prepared by diamond polished with 1µm. The etchant used to see the

microstructure was $KMnO_4$ of 4g along with NaOH in 100 ml of distilled water, to study the austenite and martensite phases another etchant was used sodium metabisulfite of 5gm and hcl of 55 ml. The sample with 20%showed maximum microhardness as compared to 26% and 36% and the reason was the occurrence of M_7C_3 type of carbides. The sample with 36% resulted in maximum corrosion resistance sample with having lowest current density as compared to other samples. Destabilization resulted in precipitation of 20% and 26% samples present in secondary carbide. The $M_{23}C_6$ and M_7C_3 both carbides were present in 26% of chromium addition sample but the 20% sample has only the M_7C_3 type and with the higher volume fraction than the 26% of the secondary carbides.

A. Wiengmoon et al. [21] explained that change occurs due to the addition of silicon on the microstructure and phase transformation operated at different temperature by using base metal as white cast iron. The SEM and XRD , the samples were tested without etching and for TEM testing, the samples gone through electropolishing and the etchant used was $BuOC_2H_4OH$ of 30% with ethanol and the perchloric acid of 10%. The silicon was added in four different proportion staring from 0.3 to 3%. The silicon samples were mostly consist of dendritic eutectic type of carbides but working on elevated temperature, the phase transformation was observed with having initial phase of M_7C_3 carbide and after transformation the carbide present was $M_{23}C_6$. The martensite also present in the sample when silicon with 1.0% added to it.

Chapter-3

Experimentation and Methodology

3.1 Materials

Hardfacing alludes to a covering method that includes welding a more consumption and wear safe material onto the surface of a less tough metal. The procedure might be performed preceding the utilization of the substrate metal or intermittently as support. As hardfacing technique tremendously used in the field of repairing of equipment for tractors, sugar mills, jcb machine, cement carrying trolleys, grain mill, dozer teeth etc. Earlier it was started with the powder to deposit on the substrate with the help of SMAW or manual arc welding but knowing about the latest technique of hardfacing, now a days the powder or the flux already mixed to make hardfaced electrodes rather than using separate power to deposit on the base metal. Different electrodes were made for coating depending upon the application. The electrodes have different mechanical properties and with distinct diameter. Procedure for the utilization of electrodes conveys that at what type of current that is AC or DC should be used for the welding operation.

3.2 Substrate (Base metal)

As per the application was the sugar mill rollers. So, the substrate was the gray cast iron as in our country almost all the sugar mill rollers are made up of this kind of cast iron. Grey cast iron has graphite flakes in its structure seen by optical microscope. These graphite flakes make the metal weak such that the change of fracture occurrence will be more in such cases. The grey cast iron has low melting point ranges from 1140 to 1200^0 C. The chemical composition for grey cast iron was given in the table below:

Table 3.1 Chemical composition of base metal

Grey Cast Iron	Carbon	Silicon	Manganese	Sulfur	Phosphorous
% age	3.35	1.85	0.73	0.18	0.08

3.3 Types of cast iron

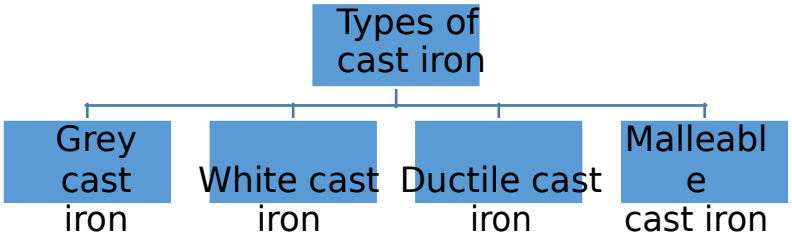

Fig 3.1 describes about types of cast iron

White cast iron This was brittle type of cast iron which showed white color cracks in the microscope after break. It has presence of carbides and these get precipitated and which results in the formation of particles which are larger than carbides and that helps in making the material hard.

Table 3.2 Chemical composition of white cast iron

Iron	C	Cr	Mn	P	Si	Mo
% age	2.4	13-17	0.4	0.14	1.2	0.6

Applications: Grinding balls, cement mixers, fabrication industrial components.

Ma**lleable cast iron** White cast iron after heat treatment known as malleable cast iron which results in the formation of graphite's and thus reduces the amount of carbides. This type of cast iron was very much similar in the properties of grey cast iron. Shrinkage in this type plays one of the important role which provided increment in the price of cast iron.

Table 3.3 Chemical composition of malleable cast iron

Iron	C	Ni	Mn	P	Si	Mo
% age	2.1-2.8	0.4-0.8	0.14-1.24	0.02-0.15	0.91-1.8	0.3-0.5

Applications: Hand tools, brackets, farming equipment, gas industry, transport industry

Ductile cast iron Nodule shape of the graphite was formed after the effect of magnesium due to reaction with oxygen and the presence of sulfur in this type of cast iron. These cast irons are much more flexible than the other kind of cast irons.

Table 3.4 Chemical composition of ductile cast iron

Iron	C	Si	Mg	P	S	Cu
% age	3.2-3.6	2.2-2.8	0.1-0.2	0.03-0.04	0.005-0.02	0.40

Applications: Pipe fittings connecting rods, cylinders, idler arms, calipers

3.4 The following steps were taken while performing the experimentation as follows:

1. First step was the collection of various elements like chromium, cerium oxide, lanthanum oxide.
2. Second step was the arrangement of the sample of grey cast iron made by casting with a dimension of 150 mm x 25mm x 15mm.
3. After samples were prepared, grooving in rectangular shape was done.
4. After completing the grooving, paste of elements were made by mixing the elements with the potassium silicate. This step was necessary to do so that the elements were properly deposit on the substrate and did not flew while doing welding operation.
5. Finally, after mixing, the grooves were filled with the paste.
6. Placing all the samples in sunlight to make the paste more dry so that welding can be done smoothly without any interrupt.

3.5 Following tests were performed for the experiment analysis

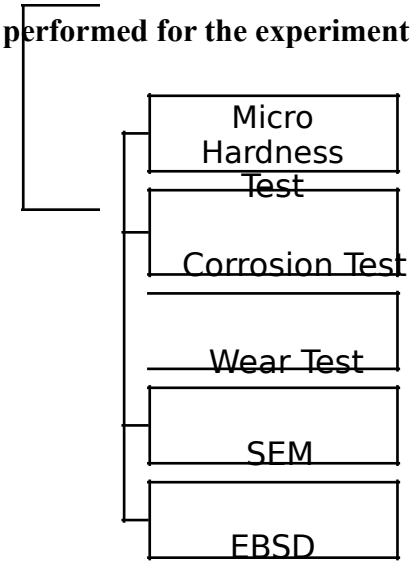

Fig 3.2 various test examined for study properties of cast iron

3.6 Chemical composition of the electrode

The composition of the base metal and the electrodes was found by using spectroscopy machine. Here the chemical composition prescribed below with table 3.4 and 3.5 respectively.

Table 3.5 (Base metal)

Iron	C%	Si%	Mn%	C.E.%	P%	S%
Grey C.I	3.15	2.01	0.7	4.0	0.20	0.25

Table 3.6 (Electrode)

Electrode	C%	Mi%	Si%	S%	Mo%	V%
Hardfaced	0.45	0.55	0.95	0.03	0.70	0.60

3.7 Material used for the welding

Five different material were deposited on the substrate which are chromium, cerium oxide, lanthanum oxide, mixer of chromium and cerium oxide, mixer of chromium and lanthanum oxide.

3.8 Fixed parameter

Here are the few parameters which should kept constant during the experimentation.

- Measurement of the sample observed 150mm x 25mm x 15mm
- Current during use of shielded manual arc welding was 150 A, Voltage was 35and AC was under use in power supply.

3.9 Sample Preparation

Before casting was done, the wooden block of dimension 150.5mm x 25.5mm x 15.5mm was prepared to cast the sample with dimension of 150mm x 25mm x 15mm as shown in figure

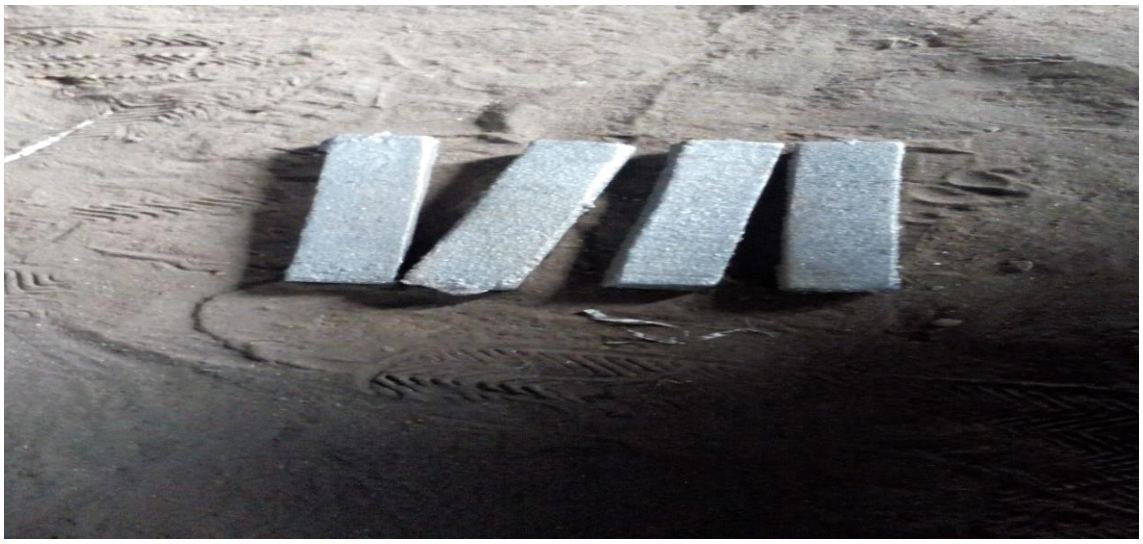

Fig 3.3 C.I. plates after casting (Courtesy R S Industries)

Equal groove was made on the casted plates with dimension of 4mm x 3mm which a rectangular shape of groove over a 150mm length of grey cast iron plates.

Fig 3.4 Grooving done on cast iron plates (Courtesy TIET workshop)

3.10 Set up for SMAW

Before staring the welding operation, samples were filled with the paste of three different elements used under five different conditions such as chromium, cerium oxide, lanthanum oxide, chromium and cerium oxide addition and last one was chromium and lanthanum oxide. After filling the

samples by adding the elements, these samples were placed under the sunlight for 2-3 hours so that paste would become dry and no interruption should take place while performing the welding operation.

Fig 3.5 SMAW machine (Courtesy TIET machine tool lab)

3.11 Testing after welding the specimen

Given below the testing that were taken place after the welding of the samples:

- Microhardness
- Corrosion testing (Salt Spray Chamber)
- EBSD(Backscattered-Diffraction)
- Wear test
- SEM

Microhardness Test

All the samples were firstly grinded under the weld grinder after grinding, they were polished by using different grit papers of different grades. Completing the polishing the samples were gone through microhardness test on Vickers hardness testing machine at load of 500gm and at dwell

time of 20 seconds. The samples were polished with the help disc polisher which helps to make the sample flatter and then samples provide accurate values for the calculating the hardness values.

Fig.3.6 Disc Polisher (Courtesy TIET machine tool lab)

Fig. 3.7 Samples for hardness testing (Courtesy TIET machine tool lab)

The microhardness machine was first invented by Smith & George during 1921. Identing take place while performing and the pyramid type shape was shown in the image of the sample.

Fig 3.8 Microhardness tester (Courtesy TIET advance measurement lab)

EBSD (Electron Backscattered Diffraction) testing

EBSD or EBSP is system used to analysis the microstructure of the material at the minimum range of nanometers through the SEM technique. The sample has dimension of 10mm of cube was made and after that electro-polishing was done to see the microstructure of the sample at different range. Some other properties like grain size up to 80nm can be detected, the ratio of the texture and the aspect was also calculated. The EBSD is limited to the amorphous material.

Fig 3.9 SEM Machine with EBSD (Courtesy IIT Bombay)

The samples both before and after the electropolishing was shown in the form of 10mm of cube. The main advantage of electropolishing was that it does not requires etchant to use to the structure.

Fig 3.10 (a) Without polishing (b) With Polishing (Courtesy IIT Bombay, Metallurgical engineering & Material science lab)

Wear Test

Wear test done on the pin-on-disc by varying different parameters like sliding distance, load at constant velocity of 2m/s and time interval of 5 minutes to calculate the weight loss for the samples. The samples with dimension of 10mm cube was prepared in such a manner that the weld bead was bit larger than the surface of the base metal as shown in figure below. The samples were rubbed on grit paper of 600 grade so that proper flat surface was made, and less vibration will take place during the operation. To start with the wear test various necessary things to be done before the testing which includes the making of disc which should be harder than the base metal which was used. So, for this experiment the disc of steel of EN31 grade used as the hardness of this was higher than the grey cast iron samples disc having a diameter of 125mm and the tempering was also done to increase its hardness. The weighting machine should be there as shown in the Fig 3.13 to measure the sample weight before and after testing.

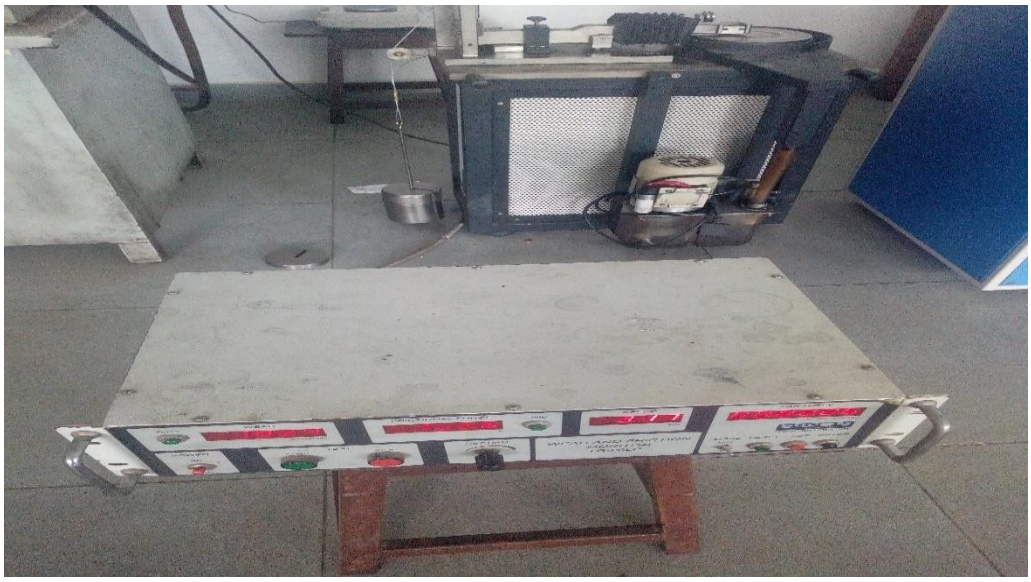

Fig 3.11 Pin on disc machine (Courtesy TIET machine tool lab)

Shape of the samples prepared for the wear was shown down in the Fig 3.12. The samples were prepared in such a way that the weld bead portion was enlarge than the base metal so that the weld bead can be easily rubbed on the disc of EN 31 steel.

Fig 3.12 Two different sides of samples (Courtesy TIET workshop)

Each sample was weighted before and after the wear test take place to know about the mass loss by using weighting machine of small units upto 200gm capacity. Theweighting machine was shown below.

Fig 3.13 Weighing balance (Courtesy TIET machine tool lab)

SEM Analysis (Scanning Electron Microscope)

SEM was invented in 1937 by German physicist who made around 600 patents. SEM is used for the analyzing the microstructure of the various material. By this technique different microstructure can be observed at higher magnification. The sign made from electron specimen interactions provide the study of texture, composition and orientation of the material. SEM also generates the structure analysis at particular point. Polished and unpolished, both the samples were possible to see the microstructure. Polishing of the samples can be done by different method such as by using emery papers of distinct grades starting from 200 to 2000, secondly by the diamond polishing and thirdly by the electropolishing. Polished sample requires etching. So different etchants can be used for the etching the samples depending upon the material. For the cast iron nital or perchloric acid was used to see microstructure of the samples. The volume of nital for cast iron was 4 %, picric acid and perchloric acid shown in the Table 3.7, Table 3.8 and Table 3.9.

Table 3.7 Nital (Etchant)

Etchant	Concentration	Condition
Nital (Ethanol+HNO_3)	Ethanol=100ml HNO_3=1-10ml	Seconds to minutes

Table 3.8 Methanol & perchloric acid

Etchanl	Concentration	Condition
Methanol+ Perchloric acid	Methanol= 80ml Perchloric=20ml	Second to minutes

Table 3.9 Picral

Etchant	Concentration	Condition
Picral	Ethanol=100ml Picric acid=2-4ml	Seconds to minutes

Fig 3.14 SEM machine (Courtesy SAI lab TIET)

Corrosion Testing

Corrosion testing done by having the samples under the salt spray chamber for 96 hours (time can be varied). The samples were placed in NaCl of 5% solution having ph value varies from 6.4 to 7.2 which makes the environment more corrosive. After every 24 hours samples were checked and the status for all the samples were updated and image of the corroded sample was taken while inspecting the samples after 24 hours. After the completion of the corrosion testing, all the sample were gone through the SEM testing just to see the microstructure and to know about the type of corrosion took placed.

Fig 3.15 Salt spray chamber (Courtesy Alpha test house, Mohali)

Chapter 4

Results and Discussions

4.3 EBSD (Electron backscattered diffraction)

The main function of EBSD is to determine the detail of microstructure parameters such as grain size, crystal structure, and chemical composition of alloying, phase diagram and the defects like porosity of the sample was found. Talking about the grain orientation, the crystal were found in the shape of cubes and each color of the cube shows the area acquired by the grain size as shown in figure 4.1. The grain boundaries having high angle & low angle boundaries. The recrystallization process work under the grain boundaries. This recommends it merits knowing something about the structure and properties of limits. Color of grain depends upon the crystal direction.

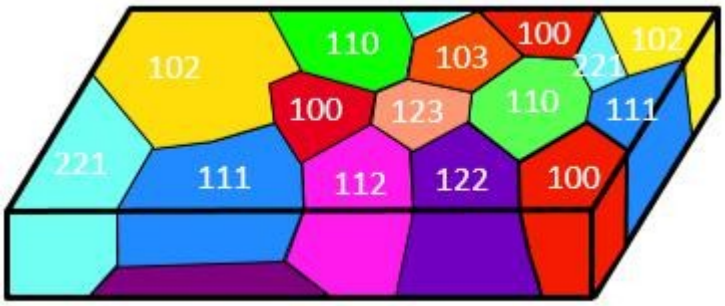

Fig. 4.1 Grain orientation

Five diffreent material sample were performed the EBSD analysis and the microstructure is shown which describe the grain size of the different crystals present in the samples and also the misorientaion of the angle with a number of fractions. Each color describe the single grain present in microstructure.

Chromium alloy

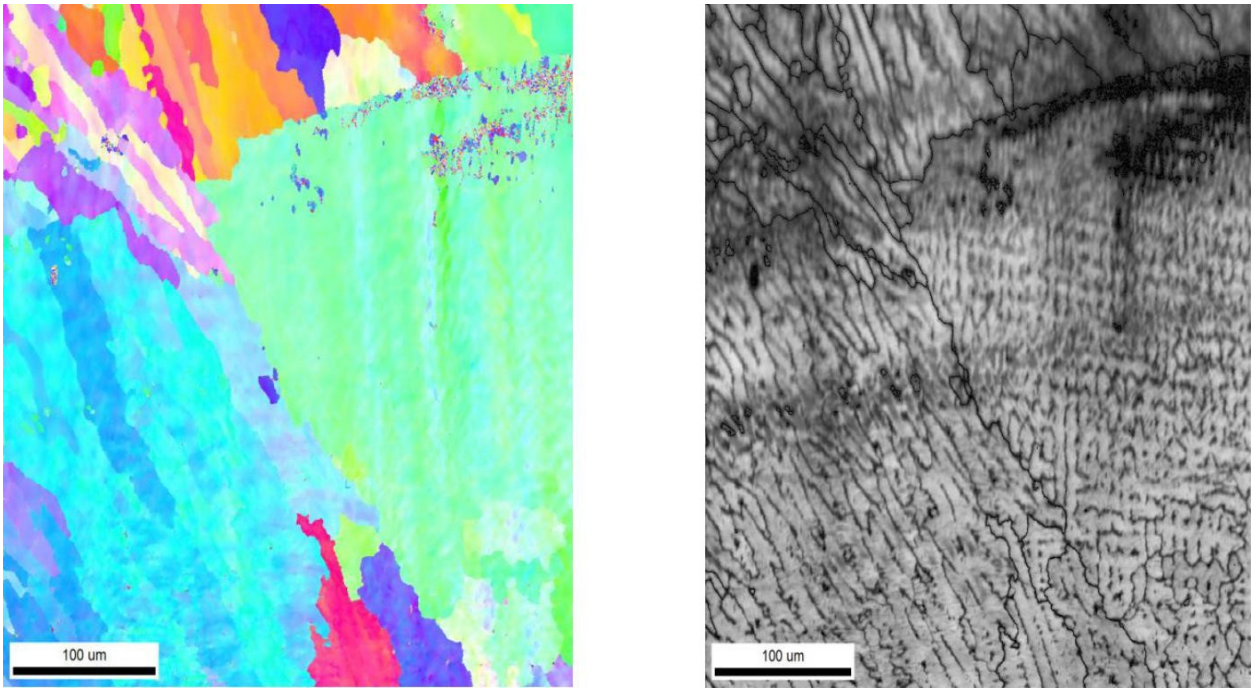

Fig. 4.2 (a)Grain color diagram (b) map of grain present

Cerium oxide alloy

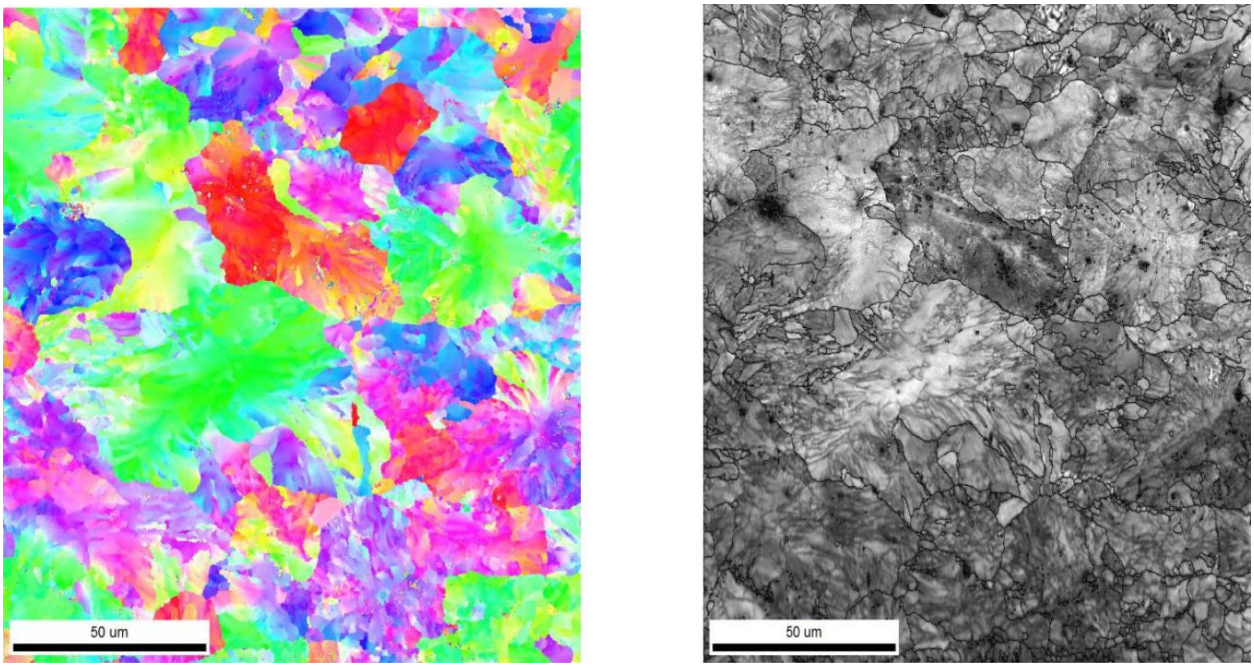

Fig. 4.3 (a) color map for CeO_2 (b) Grain Structure with sharp edges

Lanthanum Oxide alloy

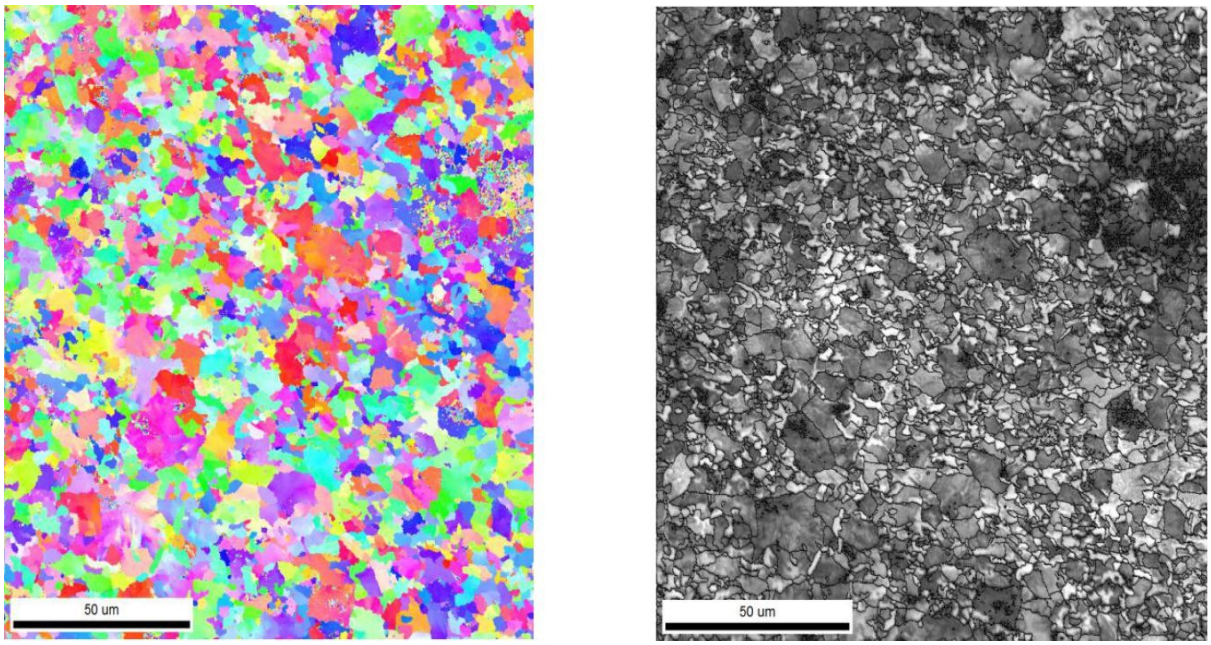

Fig. 4.4 (a) La_2O_3 color grain boundaries (b) Microstructure for La_2O_3

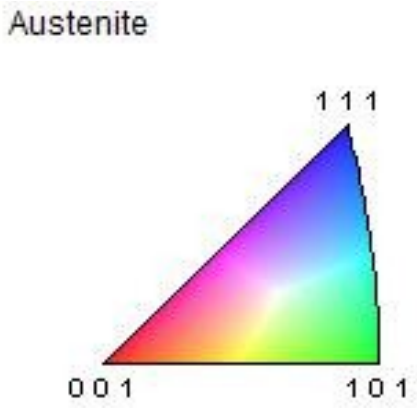

Fig. 4.5 Position of the grain with the colors

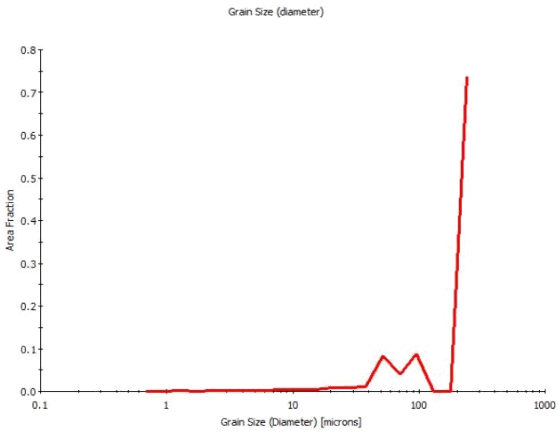

Chart: Grain Size (diameter)

Edge grains included in analysis

Diameter [microns]	Area Fraction
0.692915	0.000415611
0.942865	0.000691218
1.28298	0.00144583
1.74578	0.000853236
2.37552	0.00110507
3.23242	0.00154181
4.39843	0.00168358
5.98504	0.00124067
8.14397	0.00357144
11.0817	0.00527175
15.0791	0.00445814
20.5185	0.00812644
27.9199	0.0092588
37.9913	0.0115403
51.6956	0.0837395
70.3433	0.0397966
95.7178	0.0882496
130.245	0
177.228	0
241.158	0.73701

Average	
Number	3.37403
Area	217.025
Standard Deviation	
Number	15.9258
Area	110.637

Fig. 4.6 Plot between grain size and area fraction & chart for grain size

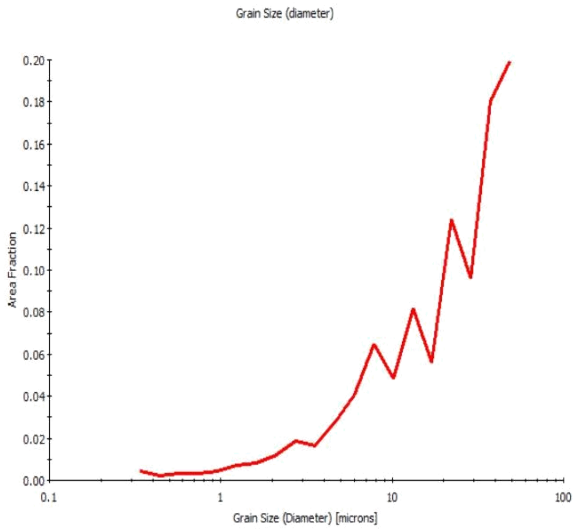

Chart: Grain Size (diameter)

Edge grains included in analysis

Diameter [microns]	Area Fraction
0.338482	0.00426165
0.439618	0.00229426
0.570972	0.00340498
0.741574	0.00342202
0.963151	0.00452035
1.25093	0.00701445
1.6247	0.0081639
2.11015	0.012156
2.74065	0.0188281
3.55954	0.0165989
4.6231	0.0276488
6.00445	0.0405066
7.79853	0.0649146
10.1287	0.0484071
13.155	0.0820309
17.0857	0.0558212
22.1908	0.124176
28.8212	0.0961512
37.4327	0.180442
48.6174	0.199236

Average	
Number	1.20498
Area	26.4602

Standard Deviation	
Number	3.01602
Area	17.5685

Fig. 4.7 Graph plot for CeO_2 and grain size chart

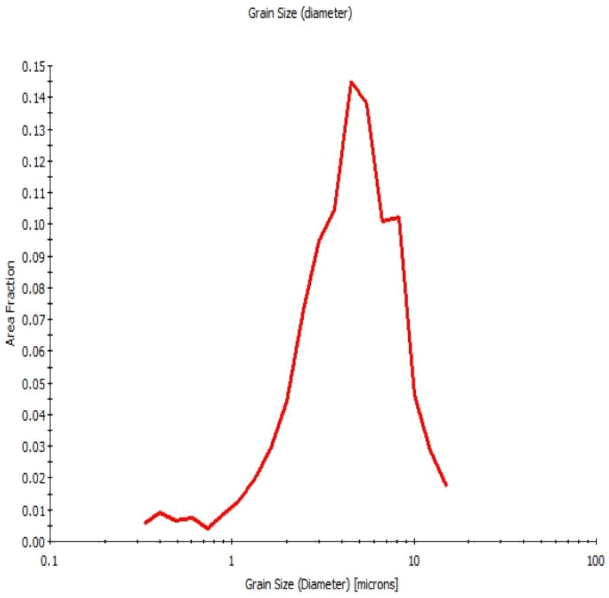

Chart: Grain Size (diameter)

Edge grains included in analysis

Diameter [microns]	Area Fraction
0.328437	0.00597451
0.401629	0.00888001
0.491132	0.00653423
0.60058	0.00757034
0.734419	0.00429222
0.898084	0.00870078
1.09822	0.0129553
1.34296	0.020109
1.64224	0.029566
2.00821	0.0440903
2.45574	0.0730777
3.003	0.0946505
3.67221	0.104582
4.49056	0.14502
5.49128	0.138065
6.71501	0.101166
8.21144	0.102246
10.0414	0.0460761
12.2791	0.0289937
15.0155	0.0174503
Average	
Number	1.17262
Area	5.02981
Standard Deviation	
Number	1.45992
Area	2.96236

Fig. 4.8 Graph Plot for Grain size and Grain size chart

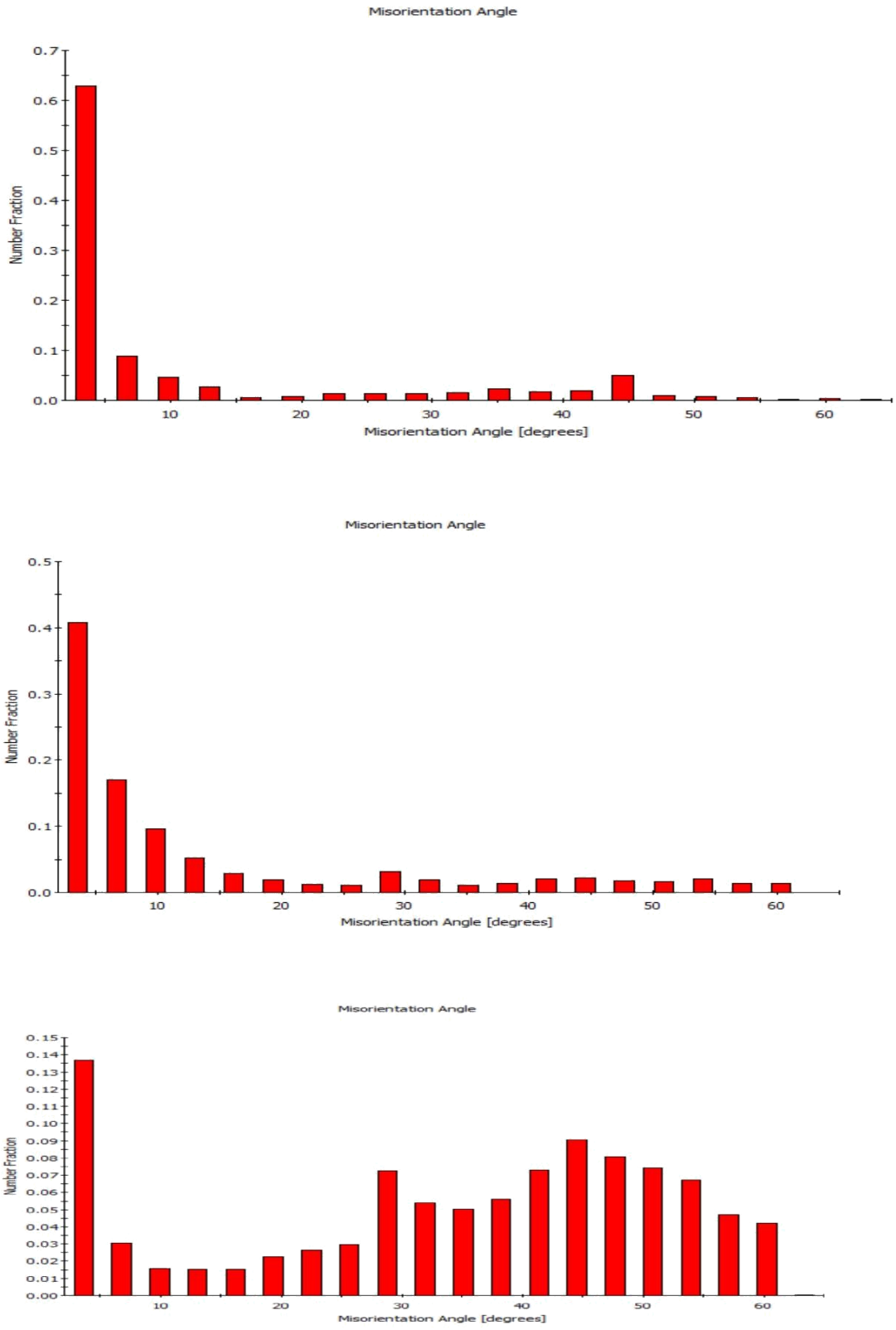

Fig. 4.9 Graph plot for misorientation for (a) Cr, (b) CeO_2, (c) La_2O_3

Results & Discussions of three samples

All the above images shows the microstructure of all the three different alloys along with their graph plot between the area fractions to grain size. One table of average mean and standard deviation of all three alloys were shown. Detail of the crystalline microstructure was shown along with graph and average size of grain.

Chromium firstly the crystalline microstructure of chromium was homogeneous microstructure as it shows no precipitates present in it. AS the structure states that the grain size of the crystal cubes are very large. Grain size mentioned with distinct colors and secondly the average grain size was found to be 217 with a standard deviation of 111. The grain size plays important role to know about the potential failure or the development of properties of cast iron samples. It was clear from the chart figure that up to 10 micron of diameter there was very less increase, up to 51 μm, it showed increase in number of area fraction and after this value it again dropped at 70 μm and this stage it was seen that at 95 μm, the value increased .On the other side the misorientation with large bars explains the presence of the twin boundaries, these boundaries are with very sharp edges present in microstructure. The misorientation graph showed the maximum misorientation in chromium was at angle of 3.4. Misorientation was nothing just the misalignment between the two grains. The graphs explains that maximum number of grains present at an angle of 3.4 and the least number of grains present at an angle of 63.

Cerium Oxide this Recrystallize microstructure shows small grain boundaries as compared to the chromium alloy. It also shows the presence of the ferrite with a bcc structure. The grain size was 26 with standard deviation of 18. The grain size chart explains the first drop in size was experience at 2.7 μm and second drop at 22 μm and last drop was at 29μm and this the number of area fraction was gradually increasing. The last one was the misorientation graph which tells the presence of twin boundaries at the angle of 3.4 with number fraction of 0.40. The maximum number of grain boundaries were formed at 3.4 angle as shown in graph of misalignment of the grains. The least number of grains were present at 63 angle with a value of 0.00011.

Lanthanum Oxide as Lanthanum and cerium both are the rare earth oxides commonly used for corrosion resistance on cast iron and mild steels. Refinement of grains was seen. Lanthanum shows a very tiny grain size of 5 with standard deviation of 3. The maximum number of area fraction was 0.14 at grain diameter of 4.4 μm. After this the grain size dropped with the increase in the diameter of grain size. Among three samples which are chromium, cerium oxide and lanthanum oxide, the least grain size was of lanthanum oxide sample. The misorientation graph showed tiny boundaries at an angle of 3.4, 45, 48 and 50. This sample has large number of tiny boundaries with no precipitation present in its microstructure. The maximum number of grains formed at an angle of 3.4 with a value of 0.13 and the second most viewed grain at an angle of 41. The lanthanum has ferrite present in it with fcc structure as chromium showed large grain number and not a refined type of structure whereas the lanthanum showed small grain size number as compared the on other two samples one was chromium and other was the cerium oxide and chromium. Among these three samples the hardness of chromium sample was at the peak where other samples showed less comparatively. The misorientation graphs showed that the lanthanum has large number of grain boundaries at larger angle from 30 to 60 degree and also twin boundaries at 3.4 degree angle and some of the twin boundaries and chromium twin boundaries at 3.4 degree and the third one showed twin boundaries at the same angle shown by chromium sample.

Now here are the results of two different samples with mixture of chromium and cerium oxide and second one was chromium mixture with lanthanum oxide.

Chromium & Cerium Oxide

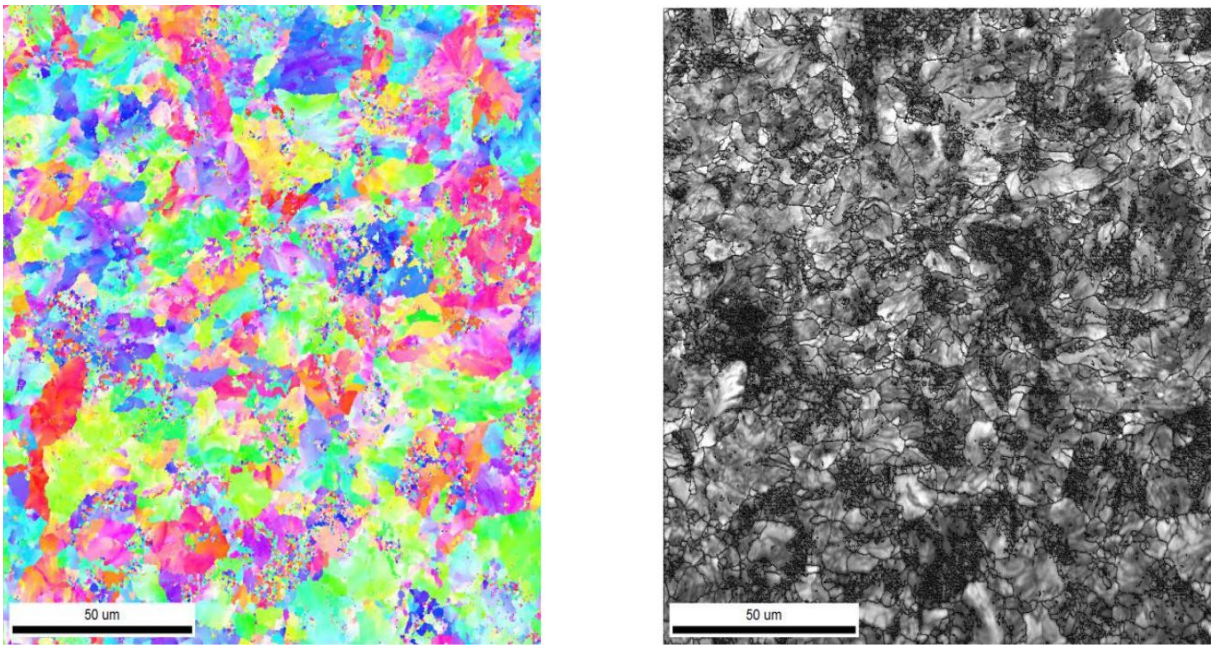

Fig. 4.10 (a) Color map of grain boundaries (b) Grain Structure

Chromium & Lanthanum oxide

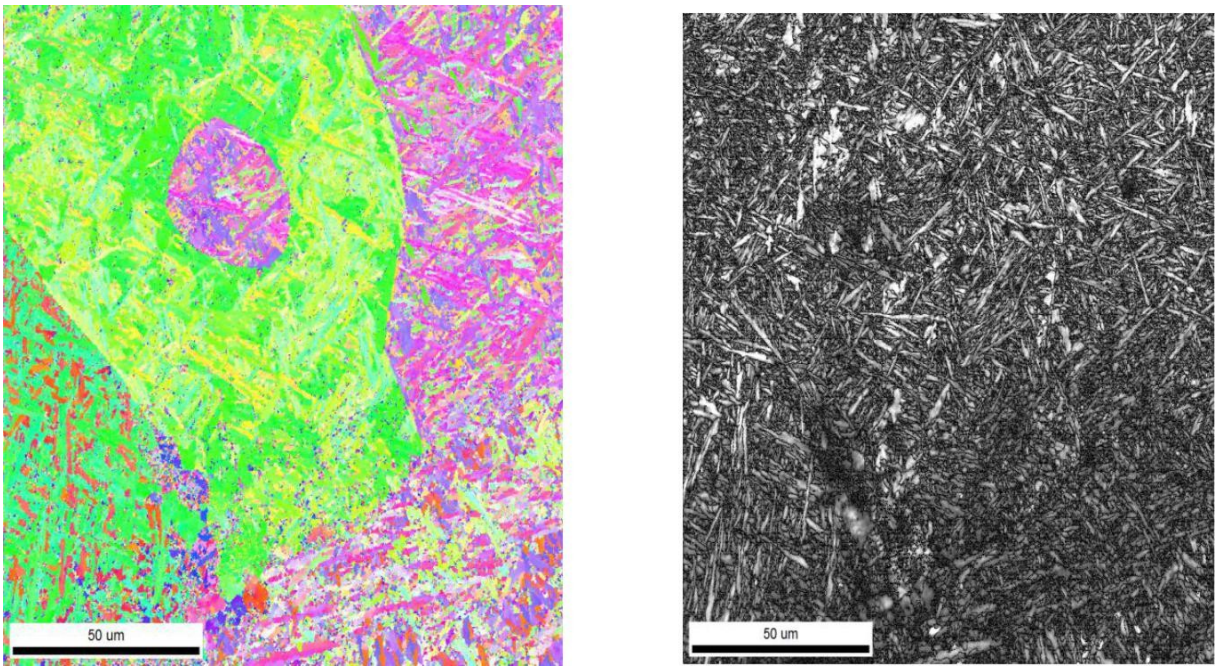

Fig 4.11 (a) Grain map microstructure (b) Grain microstructure

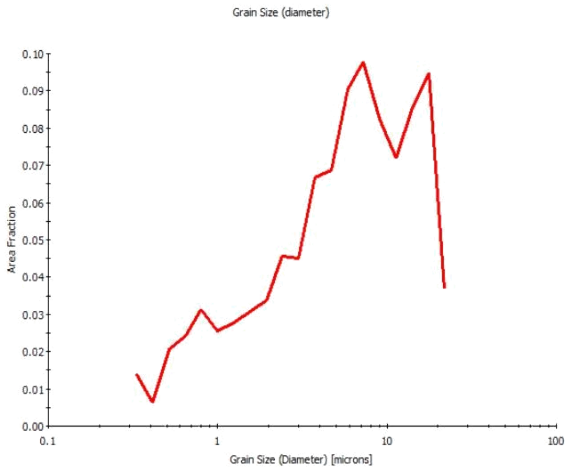

Chart: Grain Size (diameter)

Edge grains included in analysis

Diameter [microns]	Area Fraction
0.331637	0.0138962
0.413485	0.00631188
0.515532	0.0205845
0.642763	0.0242554
0.801396	0.0314066
0.999178	0.0255672
1.24577	0.0276869
1.55323	0.030635
1.93656	0.0338555
2.4145	0.0455454
3.01039	0.0451548
3.75335	0.0666716
4.67966	0.0686716
5.83459	0.0904687
7.27456	0.097916
9.0699	0.082456
11.3083	0.0719819
14.0992	0.0854876
17.5788	0.094694
21.9173	0.0367532

Average	
Number	0.857327
Area	7.53604
Standard Deviation	
Number	1.22354
Area	6.00132

Fig. 4.12 Plot for grain size and area fraction and chart diagram

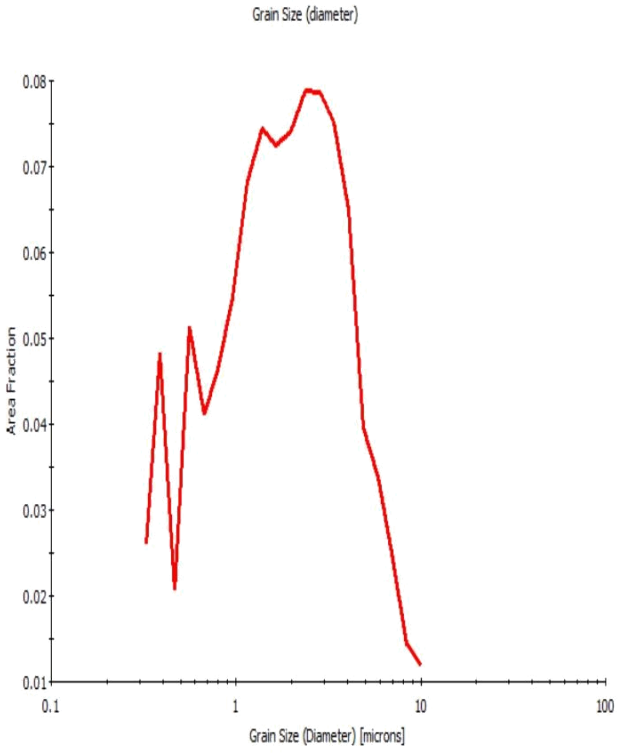

Chart: Grain Size (diameter)

Edge grains included in analysis

Diameter [microns]	Area Fraction
0.32504	0.0259153
0.389295	0.0482154
0.466253	0.0205422
0.558424	0.0512976
0.668816	0.0412202
0.80103	0.0463814
0.959382	0.0548664
1.14904	0.0682031
1.37618	0.0744154
1.64823	0.0725681
1.97406	0.0740115
2.36431	0.078754
2.83169	0.0786613
3.39147	0.0752745
4.06192	0.0649571
4.8649	0.0396195
5.82661	0.0337697
6.97844	0.0250777
8.35797	0.0143978
10.0102	0.0118519
Average	
Number	0.658146
Area	2.35563
Standard Deviation	
Number	0.591752
Area	1.94488

Fig. 4.13 Plot for grain size vs area fraction and grain size chart

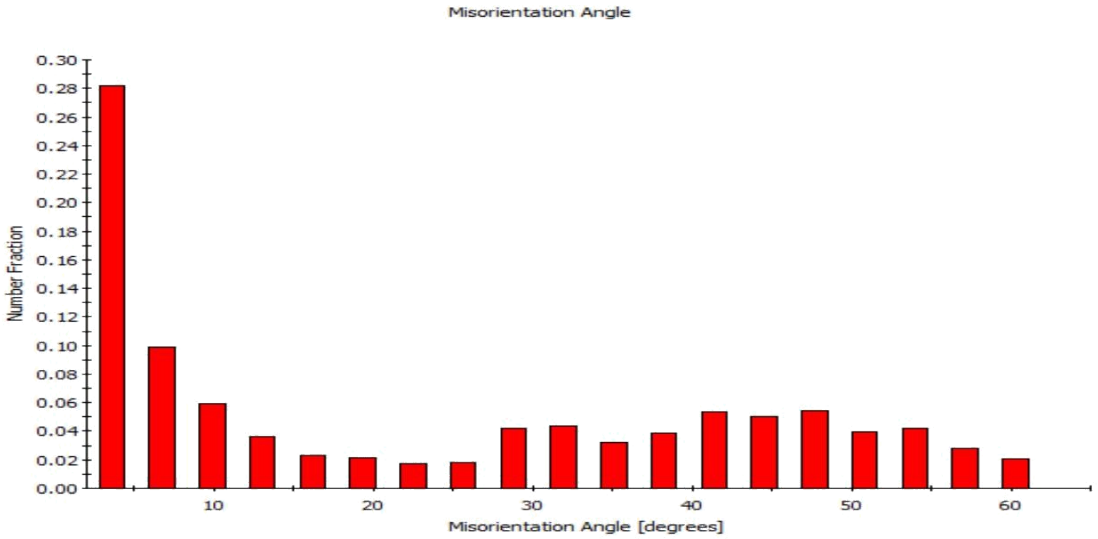

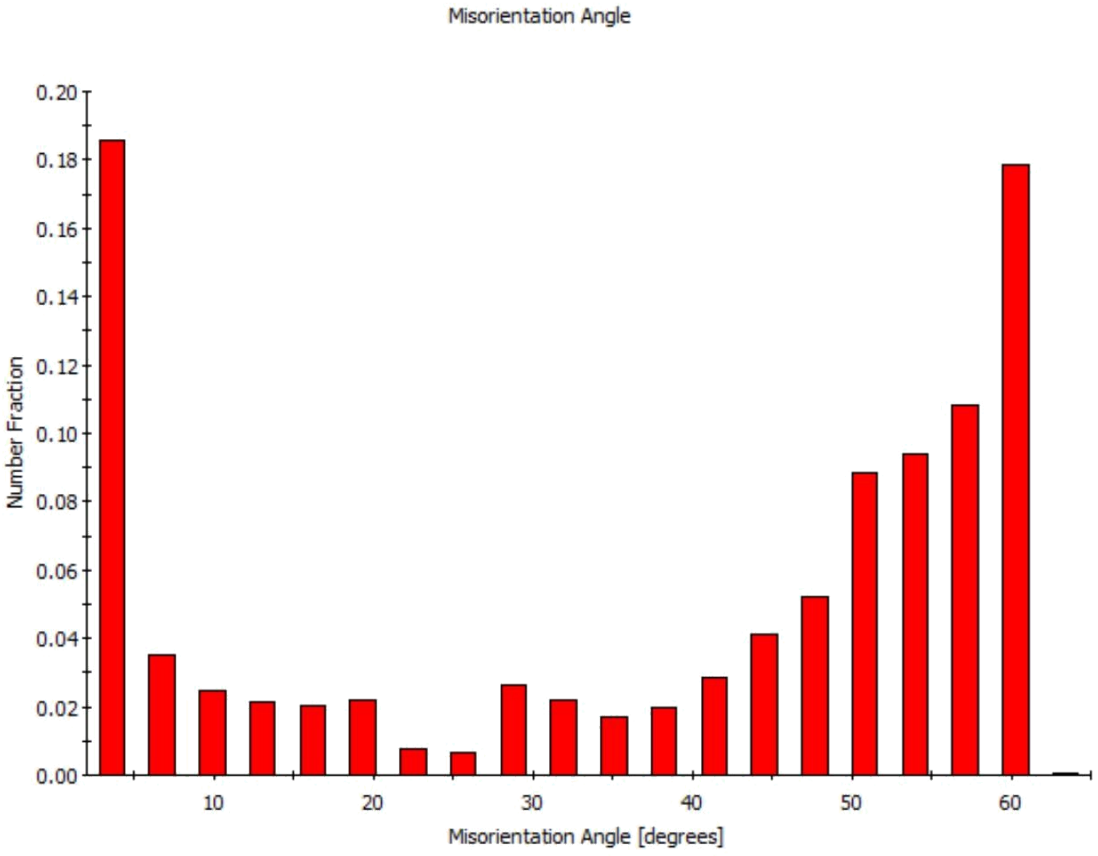

Fig. 4.14 Misorientation graph For (a) Cr + CeO_2 (b) Cr+ La_2O_3

Chromium & Cerium oxide Mixture of both these elements were tested showing homogeneous microstructure with no precipitation formed in it. The grain size was 7.53 with standard deviation of 6. Ferrite was present in this sample. The misorientaion graph represent the twin boundaries at the angle of 3.4 with highest number fraction of 0.28.

Chromium & Lanthanum oxide the recrystalline structure shows lowest grain size with value of 2.3 with a standard deviation of 2. It shows presence of pearlite. The misorienataion showed the twin boundaries one at 3.4 angle and another at 63 angle. With least grain size it also have large grain number.

4.2 Microhardness Estimations

Hardness is defined as the ability to resist the indentation and to deform the material. Vicker's hardness is one of the most common method to calculate the hardness. During the indenter provide force on the sample and it was pressed at load of 500 gm with a time of 20 seconds and after dwell is completed, the indenter come back to its original position and removing from the sample. After this the vicker's hardness number get by measuring the values of the diagonal indentation. For this operation of measuring the hardness in a correct way, sample should be uniform otherwise non uniform way will provide random values. This machine is suitable for both the soft as well as the hard material.

Table 4.1 Micro hardness

Element	Hardness(HVN)
Cr	537
CeO_2	409
La_2O_3	426
Cr + CeO_2	451
Cr + La_2O_3	544

From the above data, it was clear that Chromium and lanthanum oxide sample showed highest hardness value as compared to other four samples, it may be due to smallest grain size. The cerium oxide sample declared as the sample with least hardness value of 409. Further results should be compared with this hardness values to know more about the properties of the samples. Various

test were performed like corrosion testing, electron backscattered diffraction, scanning electron microscope and the wear test to know the effect of the different elements used on cast iron samples. The graph for the micro hardness is plotted with different values.

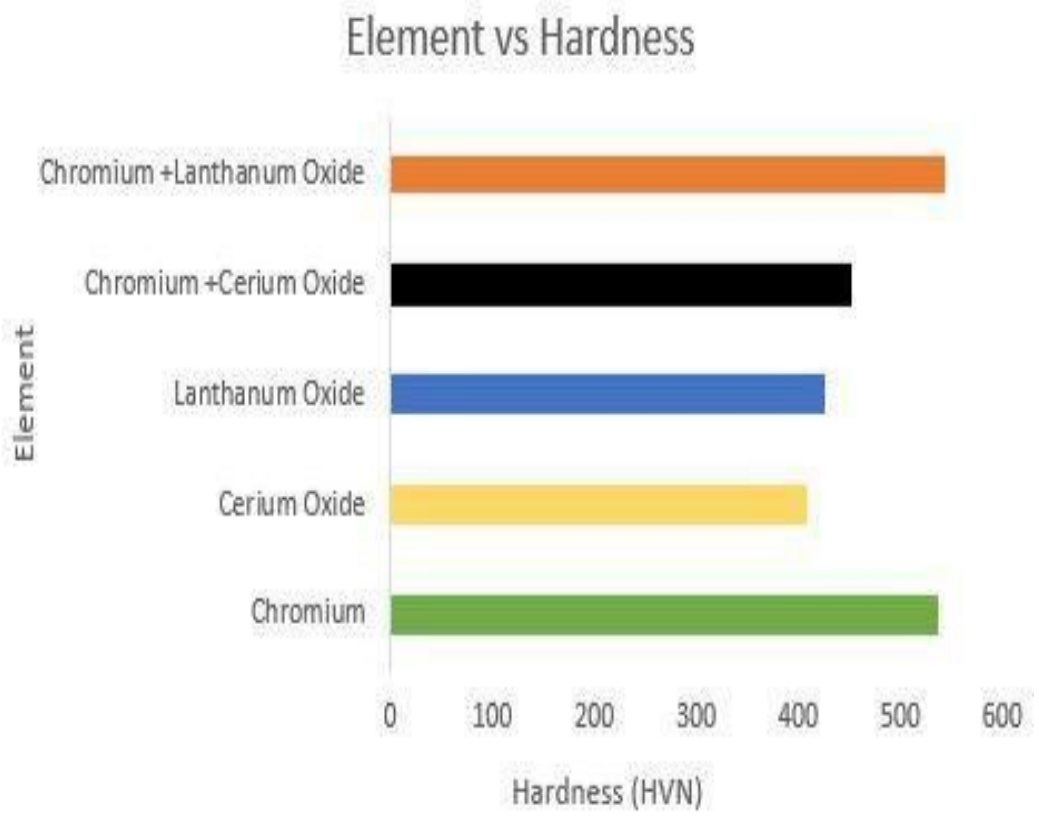

Fig. 4.15 Graph of microhardness among five samples chromium and lanthanum addition sample, chromium & cerium mixed sample, chromium, lanthanum oxide and cerium oxide sample

4.3 Wear Test Analysis

At different speed, sliding distance and load was varied from 5kg to 7.5 kg. The graphs were shown for three different samples: The time interval to weight the sample was 5 minutes, after placing sample on disc at particular rpm.

1. Chromium-Load 49.05 N, Wear track diameter 40 mm, RPM 955.

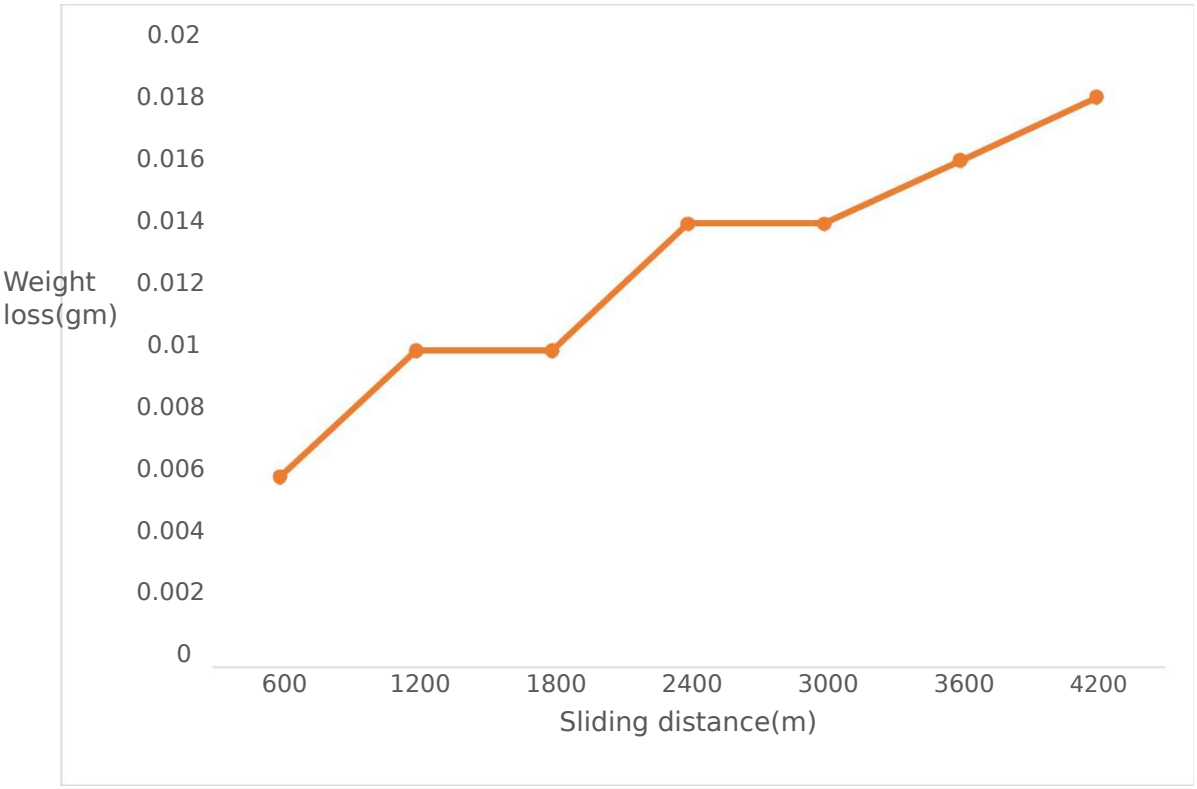

Fig. 4.16 Line Graph for Cr at 955 rpm

Figure 4.16 showed the plot between the sliding distance and the weight loss of chromium deposit sample. From the figure, it was clear that the weight loss after interval of 5 minutes at constant rotational speed of 955 rpm. First drop of weight was 6mg after 5 minutes of interval of time, for the next interval of time at 1200 sliding distance the weight drop reached 10 mg. After this interval the weight was kept constant for next 5 minutes up to sliding distance of 1800 mm. In between the 1800 to 2400 mm, the wear weight loss took place by 4 mg. From 2400 to 3000, again no loss occurred during this range of distance and after this the weight loss was 2mg while reaching at 3600 mm. At 4200 mm, the wear rate was 2mg from 3600 mm but calculating the total weight loss after completing the operation from 600 to 4200 was 24 mg on 40 mm wear track diameter and this sample provided slightly change.

2. Chromium-Load 73.575 N, Wear track diameter 70 mm, RPM 546

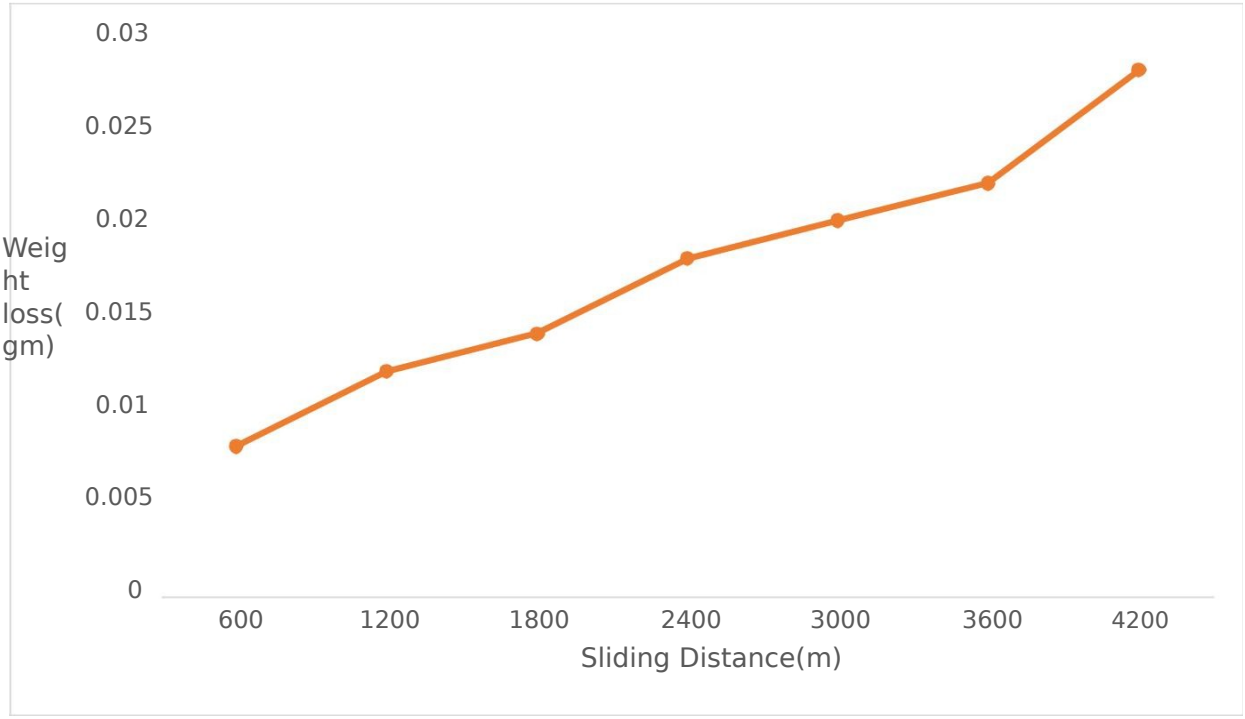

Fig. 4.17 Graph for Cr at 546 rpm

Figure 4.17 shows the plotting the chromium effect with 70 mm wear track diameter and at speed of 546 rpm with a increased load of 74.0 N. Starting with 600 mm sliding distance to 1200 mm, it was resulted that loss was 8 mg on time interval of 5 minutes. From the next distance of 1800 mm, the alloy showed decrement of 4 mg. Up to the 2400 mm of sliding distance, it declared the drop of 2 mg of weight loss which was comparatively lesser than other outcome values of the weight loss. Reached at 3000 mm, sample after gone through abrasive action, showed drop 4mg of loss which was slightly higher than last one. Again at 3600 mm, the loss was of 2 mg. At the final destination of 4200 mm of distance, it provided bit higher loss of 6 mg. As we solving the total amount of loss corresponding to the initial weight was of 28 mg. The maximiu weight loss was recorded at sliding distance in between from 600 to 1200 m and least weight loss was calculated was in between sliding distance of 1800 to 2400 m and also same weight loss resulted in between 3000 to 4200 m.

3. Chromium + Cerium Oxide- Load 49.05 N, Wear track diameter 30 mm, RPM 1273

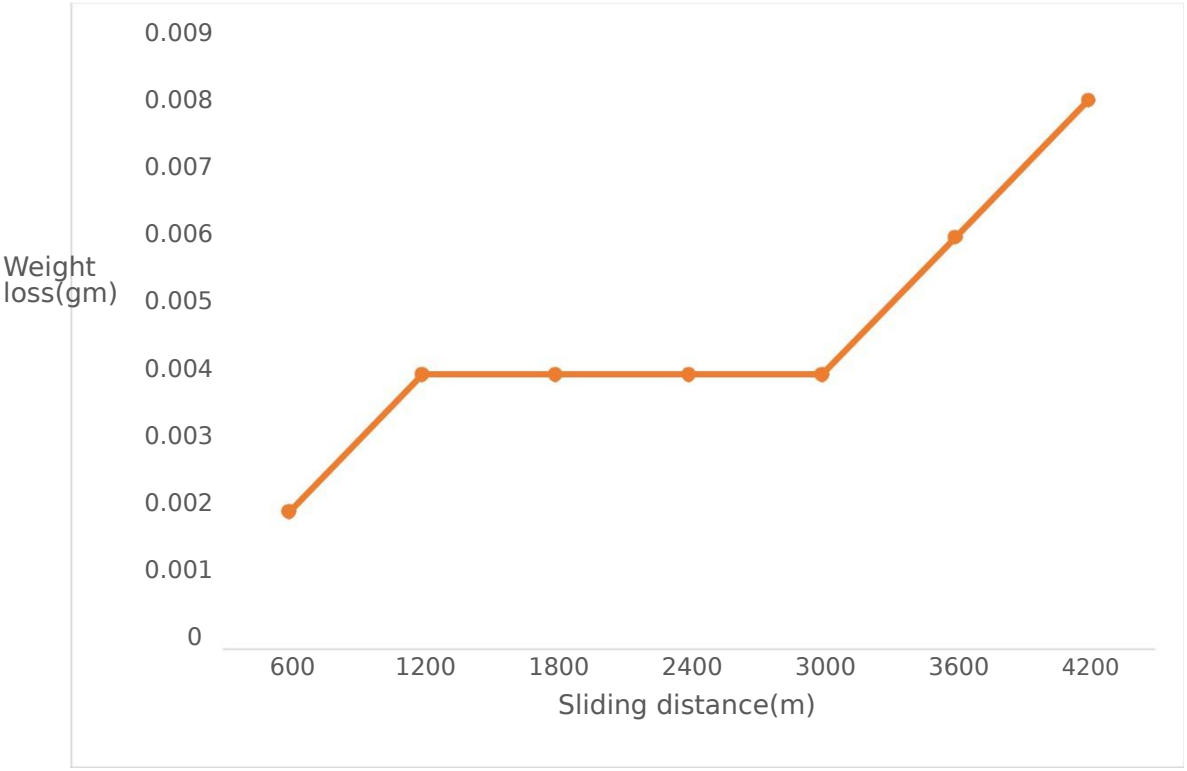

Fig. 4.18 Graph for Cr + CeO_2 at 1273 rpm

Figure 4.18 represents the graph plot for chromium and cerium oxide mixture alloy at speed of 1273 rpm and at track diameter of 40 mm. Initially weight was of 7.266 gm and the reduction was only 2 mg after 5 minutes interval of time. This 2 mg of weight loss was constant loss up to 2400 mm of sliding distance deposited against a load of 5 kg. After this time interval, the weight loss up to 3000 mm was of 2 mg and at 3600 the loss was again the same as in the previous time interval. In the last interval of time from 3600 to 4200, it was shown that same weight loss of 2 mg. But measuring the overall weight loss of chromium and cerium oxide sample was found to be of 10 mg which was slightly less than in case of chromium. This sample showed constant zero weight loss in between the sliding distance of 1200 to 3000 m. After 3000 m constant weight loss was recorded. As the microhardness does not showed any kind of co-relation between the wear resistance or the weight loss.

4. Chromium + Cerium oxide- Load 73.575 N, Wear track diameter 60 mm, RPM 637

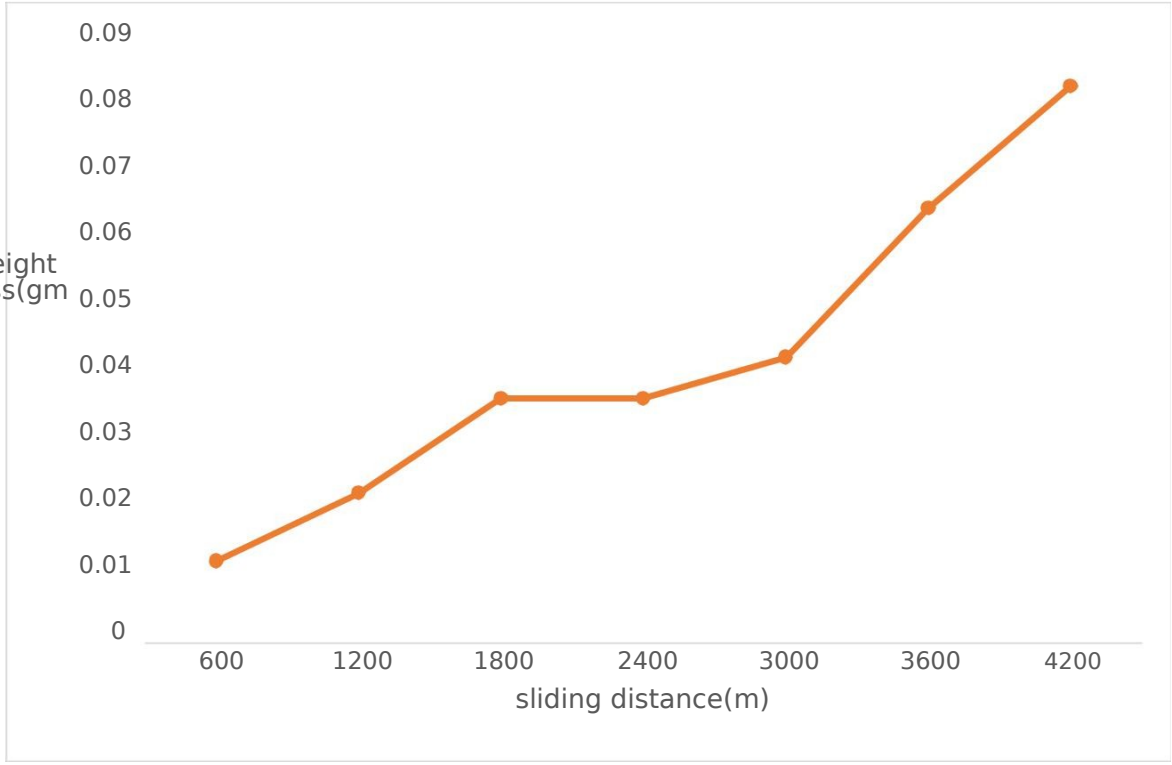

Fig. 4.19 Graph for Cr + CeO_2 at 637 rpm

Figure 4.19 examined the effect of Cr+CeO_2 deposit on cast iron sample by performing wear test and calculating weight loss with increase in sliding distance at load of 74.05 N and on 637 rpm. From the first interval, the weight loss was of 12 mg up to 1200 mm of sliding distance. During second interval the weight loss slightly decreases with 10 mg of loss. After 5 minutes of interval for the next result of loss was found to be of 14 mg at 1800 mm which was bit more than the previous result. At 2400 mm, the no loss was seen and the weight of the sample remains unchanged. From 2400 to 3000 mm, loss was 6 mg which was the lowest loss among other intervals. The weight loss was found to be of 22 mg which was the highest loss and in the last level the loss was of 20 mg at 4200 mm of sliding distance. Up to know the Chromium and cerium mixture sample provided maximum wear weight loss and the total loss was found to be of 116 mg compared to the initial weight, the last weight of sample was 7.150 gm. The wear track diameter was 60 mm in this operation.

5. Chromium + Lanthanum Oxide- Load 49.05 N, track diameter 50 mm, RPM 764

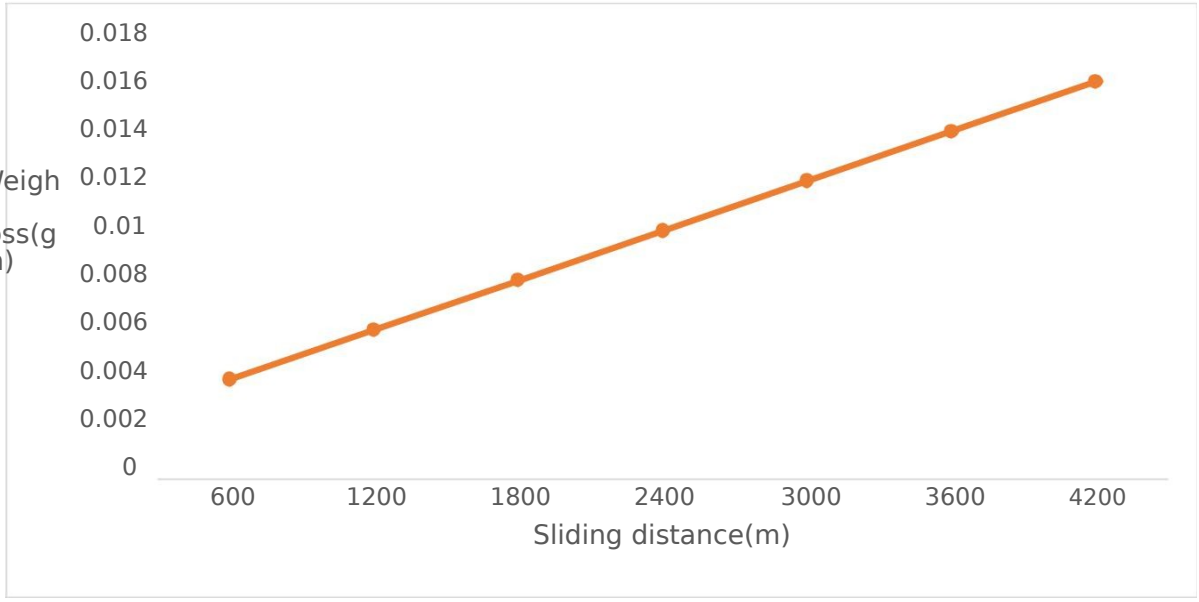

Fig. 4.20 Cr + La_2O_3 at 764 rpm

Figure 4.20 showed the graph plot for Chromium and lanthanum oxide mixture sample. Before starting, it was clear that the graph showing the straight line explained that the weight loss was constant over the entire time intervals starting from 600 mm sliding distance to 1200 mm sliding distance. The total loss from the initial weight of 6.646 gm.

6. Chromium + Lanthanum Oxide- Load- 73.525 N, Track diameter 80 mm, RPM 477

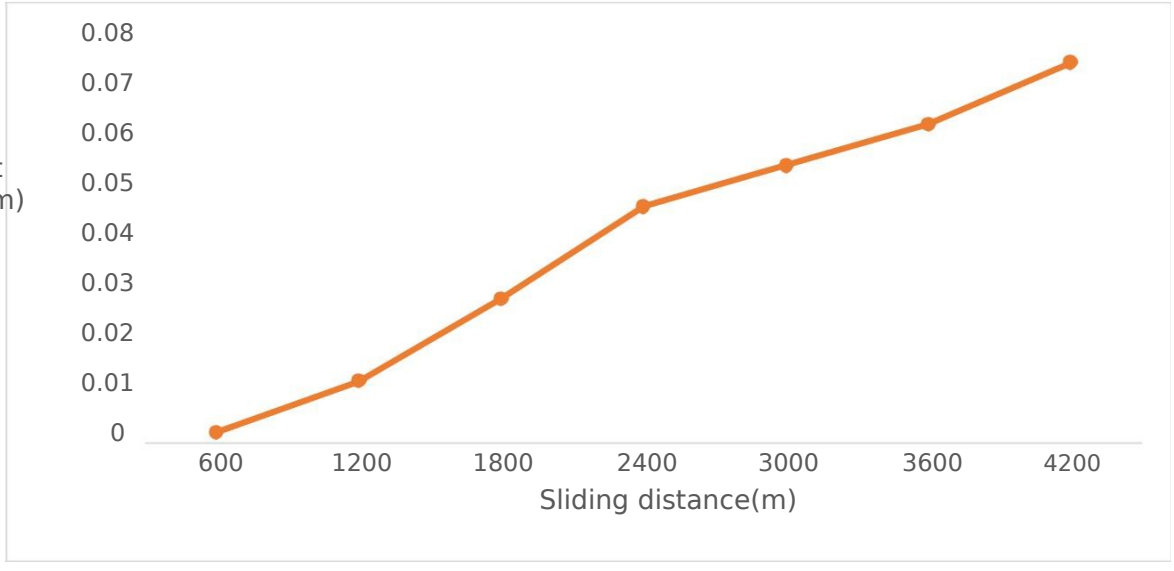

Fig. 4.21 Cr + La_2O_3 at 477

Figure 4.21 represent graph for chromium and lanthanum oxide at load of 74.05 N and wear track diameter of 80 mm and at 477 rpm the sample was rotated on disc of EN 31 steel grades. The time interval to check the weight loss was of 5 minutes. In the first stage the weight loss was 2 mg. The second interval showed that drop of 16 mg at the end of 1800 mm. The next drop after 5 minutes was 18 mg at 2400 mm. After this stage the weight was decrease by 8 mg and it was constant for next interval of time for 3600 mm. At the end, the weight drop was of 12 mg.

Discussion for wear analysis

The maximum wear weight loss was given by the chromium and cerium oxide sample whereas the least wear weight loss was given by chromium deposited samples with a value of 48 gm weight loss. The wear was more due to the load but with increase in the velocity, it showed very less change in the weight loss values. From the calculated data, the chromium deposit sample showed weight loss of 18 mg at load of 49 N along with wear track diameter of 40mm and 955 rpm, second sample of chromium resulted in weight loss of 28 mg at load of 73.05 N. The wear weight loss was high at chromium and cerium oxide mixture sample with value of 106 mg on wear track diameter 60 and at 637 rpm. The second highest weight loss was of chromium and lanthanum oxide at track diameter of 80 mm and at 477 rpm. From the above analysis data it was examined that the chromium showed

4.4 Corrosion Test & Results

For this performance of testing, the salt spray chamber is used for calculate the corrosion on cast iron samples by placing them for 120 hours that was about 5 days in a salt spray chamber. In this salt spray chamber the nozzle which is made up of tungsten, sprays the Nacl solution on the samples and the reason for using the Nacl solution as we know that Nacl was more corrosive to cast iron plates rather than Kcl, $CaCO_3$, and NaNO3. The concentration of the Solution (Nacl) used in salt spray chamber was 5g/lt and with pH value of 7.03. The corrosion rate of Nacl solution was 3.03 mpy which was highest rather than other salts values.

Parameter: Temperature = 29±2^0 C, Relative Humidity = 95±2 %

Table 4.2 Chromium addition sample

S. No.	Test Parameters	Results	Method Reference
1	Zero Hours	No sign of white or yellow spots	ASTM-B-117-11
2	After 24 Hours	No sign of white or yellow spots	ASTM-B-117-11
3	After 48 Hours	No sign of white or yellow spots	ASTM-B-117-11
4	After 72 Hours	No sign of white or yellow spots	ASTM-B-117-11
5	After 96 Hours	0 to 5% yellow spots	ASTM-B-117-11
6	After 120 Hours	20 % white + yellow Spots	ASTM-B-117-11

Table 4.3 Cerium Oxide addition sample

S. No.	Test Parameters	Results	Method Reference
1	Zero Hours	No sign of white or yellow spots	ASTM-B-117-11
2	After 24 Hours	No sign of white or yellow spots	ASTM-B-117-11
3	After 48 Hours	No sign of white or yellow spots	ASTM-B-117-11
4	After 72 Hours	No sign of white or yellow spots	ASTM-B-117-11
5	After 96 Hours	10-15 % Red + Black spots	ASTM-B-117-11
6	After 120 Hours	40-50 % Red + Black spots	ASTM-B-117-11

Table 4.4 Chromium + Cerium Oxide sample

S. No.	Test Parameters	Results	Method Reference
1	Zero Hours	No sign of white or yellow spots	ASTM-B-117-11
2	After 24 Hours	No sign of white or yellow spots	ASTM-B-117-11
3	After 48 Hours	So sign of white or yellow spots	ASTM-B-117-11
4	After 72 Hours	No sign of white or yellow spots	ASTM-B-117-11
5	After 96 Hours	0-5 % Yellow spots	ASTM-B-117-11
6	After 120 Hours	18% White + Yellow spots	ASTM-B-117-11

Table 4.5 Chromium + Lanthanum Oxide sample

S. No.	Test Parameters	Results	Method Reference
1	Zero Hours	No sign of white or yellow spots	ASTM-B-117-11
2	After 24 Hours	No sign of white or yellow spots	ASTM-B-117-11
3	After 48 Hours	So sign of white or yellow spots	ASTM-B-117-11
4	After 72 Hours	10-15% of white + yellow spots	ASTM-B-117-11
5	After 96 Hours	20-25% % White +Yellow spots	ASTM-B-117-11
6	After 120 Hours	60-70 % White + Yellow spots	ASTM-B-117-11

As per the table mentioned above which explained he effect of solution on every 24 hours of time period. Different images were seen as per the elements placed in salt spray chamber. From the recorded data it was very much clear that chromium and Cerium oxide addition provide least corrosion and on the other side it was also seen that the maximum corrosion was at the chromium and lanthanum oxide sample which was about 60-70 % of the corroded area was calculated after 120 hours placed in salt spray chamber. Mostly corrosion started taking after the 72 hours i.e. no sign was seen in 3 days. The next step is to draw the graph of all the elements used for corrosion testing and evaluate that which element recorded least corrosion rate. The maximum corroded area was of chromium and lanthanum oxide sample and very severe difference was seen between chromium and chromium & cerium oxide sample which was the difference of 2%. Still it was clear that to increase the corrosion resistance, chromium & cerium oxide addition sample can be used in case of chromium sample. Secondly the microhardness and the corrosion resistance does not showed any kind of co-relation between them. It was not necessary that the sample with the higher microhardness value should have high corrosion resistance. The percentage for 4 samples used on grooves of cast iron samples are cerium with 0.65%, chromium with 1.78%, chromium and cerium oxide with 1.57% and chromium and lanthanum oxide with 1.27%. The chromium weightage was more but the area of groove was same in all the sample with a dimension of 4 x 2 mm also shown images of the samples in chapter 3.

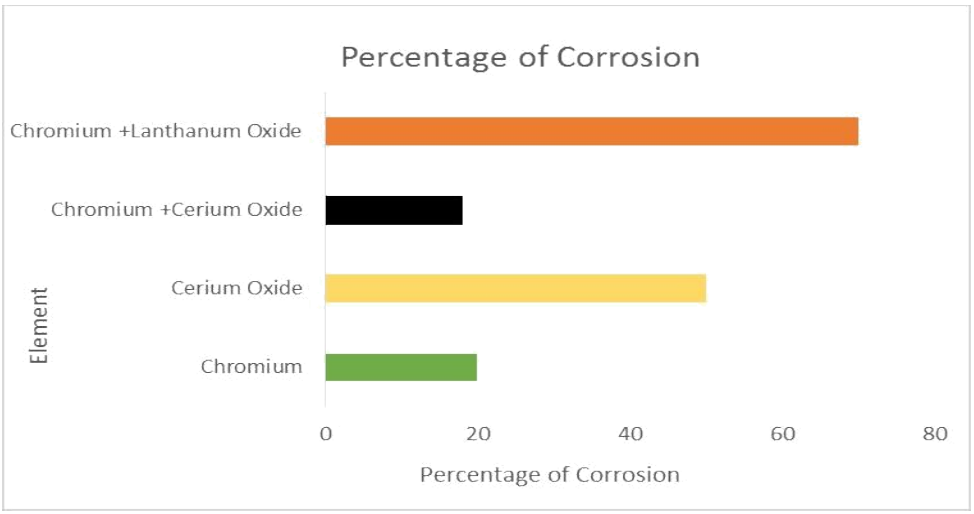

Fig. 4.22 Graph of corroded area vs elements where $Cr+CeO_2$ shows least corroded area

4.2.1 Following the images for the sample which were under the salt spray chamber for 120 hours

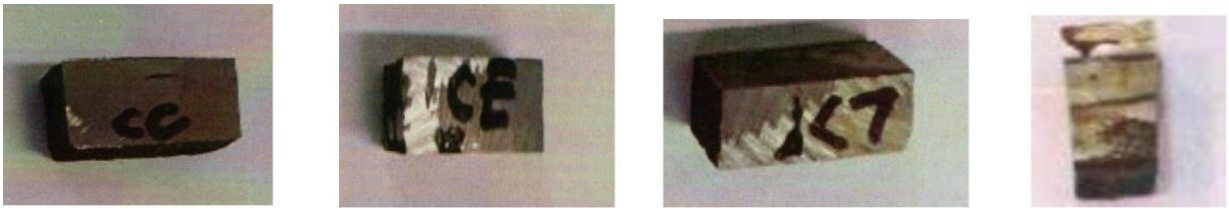

(a) Cr **(b) CeO_2** **(c) $Cr+CeO_2$** **(d)$Cr+La_2O_3$**

Fig. 4.23 Showed four samples before place under the salt spray chamber, it was seen that no corroded area was present initially at 0 hour on the samples.

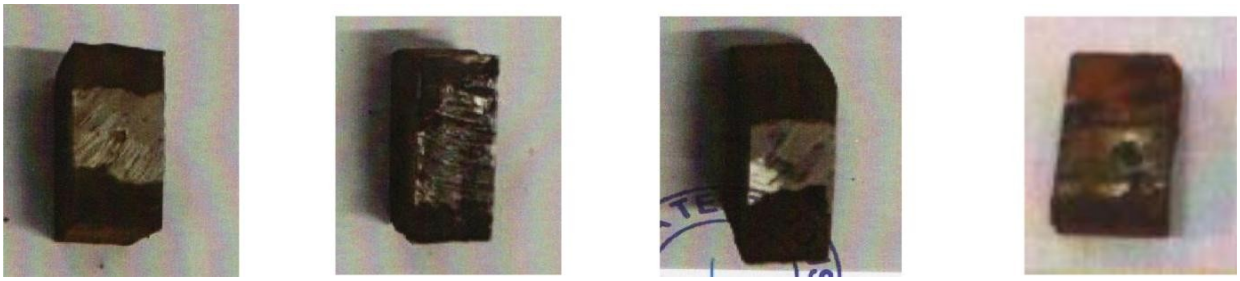

(a) Cr **(b) CeO_2** **(c) $Cr+CeO_2$** **(d) $Cr+La_2O_3$**

Fig. 4.24 shows the samples after the sample placed for 24 hours and it was observed that no sign of corrosion or spots were seen

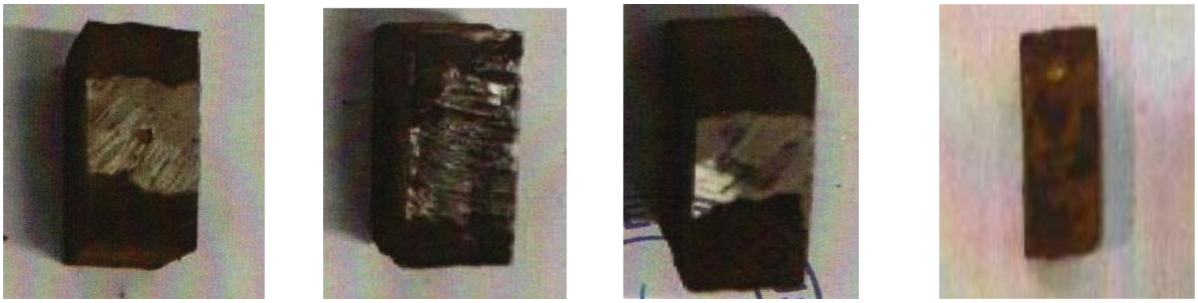

(a) Cr **(b) CeO_2** **(c) Cr+CeO_2** **(d) Cr+La_2O_3**

Fig. 4.25 shows samples 48 hours and no corrosion signs were seen among all the four samples

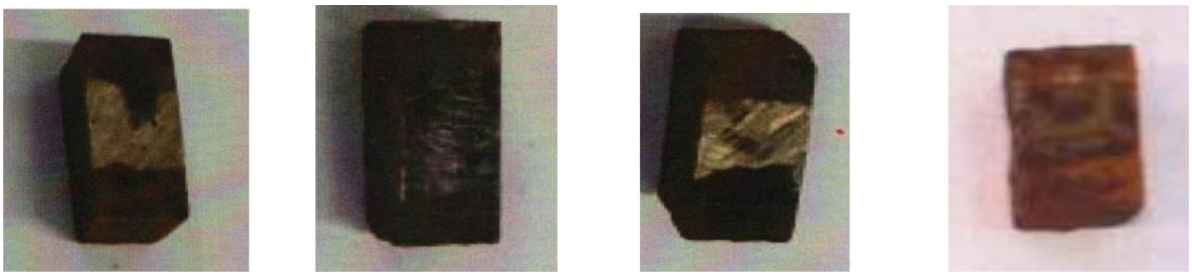

(a) Cr **(b) CeO_2** **(c) Cr+CeO_2** **(d) Cr+La_2O_3**

Fig. 4.26 showed samples after 72 hours and some yellow spots were seen at (b) and (a) samples and (d) got corroded up to 15 %

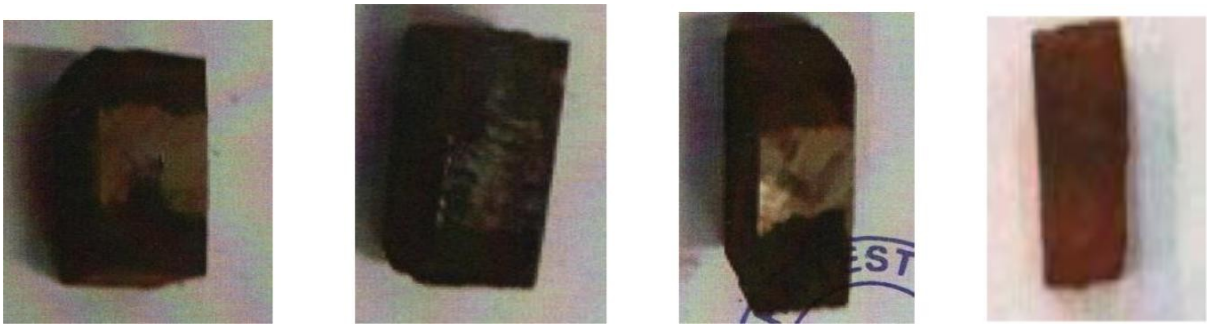

(a) Cr **(b) CeO_2** **(c) Cr+CeO_2** **(d)Cr+ La_2O_3**

Fig. 4.27 showed samples after 96 hours and some 15-20 % (b) get corroded, (a) about 5%, (c) 4% which was cerium addition sample (d) get corroded upto 35%

(a) Cr

(b) CeO_2

(c) $Cr+CeO_2$

(d) $Cr+La_2O_3$

Fig. 4.28 showed (d) as most corroded sample among other four samples and chromium and cerium addition sample showed least corrosion with corroded area of about 18 %

4.2.1 SEM images for corroded samples

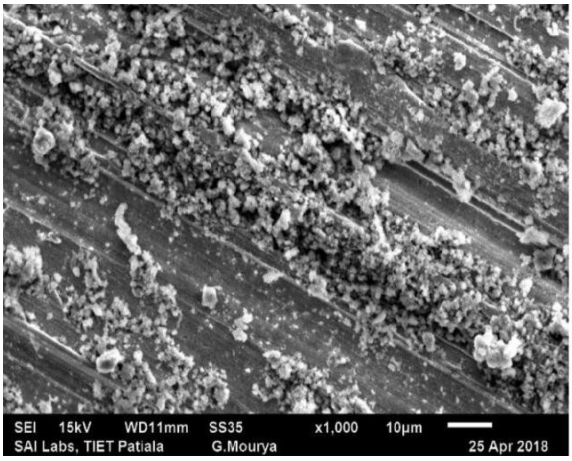

(a) Cr

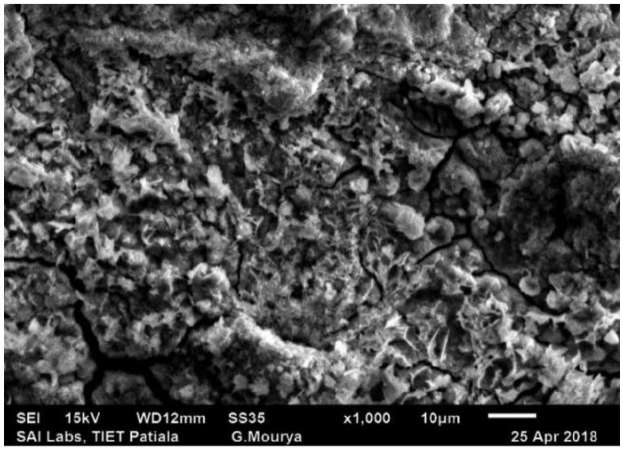

(b) $Cr+CeO_2$

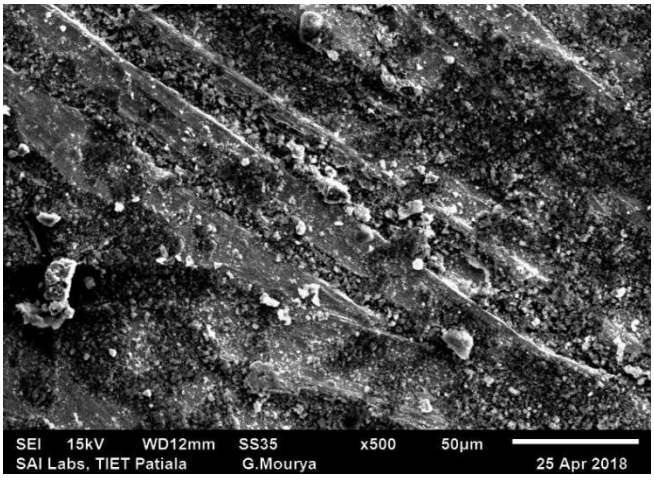

(c)$Cr+La_2O_3$

Fig. 4.29(a) showed that oxide layer formed over the surface of weld. No Distortion shown in this image

Fig. 4.29(b) showed pitting corrosion and crevice corrosion. Many holes and cavities are formed over the surface of weld bead. Weight occurred here on the surface of weld bead. Material start decompose.

Fig. 4.29(c) showed that there is no formation of oxide layer and some cotton balls like layers show on the surface of weld bead. Some delamination present in the above image.

Chapter 5

Conclusions and Future Scope

5.1 Conclusions

Five different samples were prepared with different composition of chromium with 1.78%, cerium oxide with 0.65% , lanthanum oxide with 0.4% and the mixture of cerium and chromium with 1.57% and the lanthanum & chromium sample with 1.27% and four different test were performed to know the mechanical properties of the cast iron sample**.** The following things were observed while performing the testing.

1. Chromium and lanthanum oxide (1.27%) sample showed maximum hardness as compared to the four other samples with value of 544 Vicker's hardness number. Least hardness was observed in lanthanum oxide sample with value of 409.
2. EBSD analysis showed the microstructure of five samples with grain size. Among these five samples the chromium with 1.78% showed large grain structure as compared to other samples and chromium plus lanthanum mixture sample with 1.27% showed smallest grain size of 2.35563.
3. Corrosion test took place under NaCl solution for 120 hours and it was observed that chromium and lanthanum showed least corroded area among other samples and chromium and lanthanum oxide sample showed maximum corroded area of 70 %. But the hardness does not have any direct correlation with corrosion resistance. Sometimes sample with more hardness gets more corroded than less hard sample at higher temperature.
4. Wear test analysis proved that wear resistance not proportional to hardness, it was possible that sample with more hardness will give less wear weight loss. Among five samples chromium showed least weight loss about 48 gm. On another side cerium and chromium mixture sample showed maximum weight loss.
5. Chromium and lanthanum oxide sample showed refined grain structure with least grain size with least twin boundaries present.

5.2 Scope for Future

1. In future chromium and cerium oxide can be added in the electrodes used for hardfacing for two or three layers on grey cast iron.
2. As titanium was can also be added to rare earth oxides to study the microstructure of grey cast iron and to change some mechanical properties.
3. XRD analysis can be done to know about the types of carbide present.
4. Other than shielded metal arc welding, some other weldings like submerged arc welding, plasma transferred arc welding can be used.

References

[1] ELSawy, E.E.T., EL-Hebeary, M.R. and El Mahallawi, I.S.E., 2017. Effect of manganese, silicon and chromium additions on microstructure and wear characteristics of grey cast iron for sugar industries applications. *Wear*, *390*, pp.113-124.

[2] Straffelini, G., Verma, P.C., Metinoz, I., Ciudin, R., Perricone, G. and Gialanella, S., 2016. Wear behavior of a low metallic friction material dry sliding against a cast iron disc: role of the heat-treatment of the disc. *Wear*, *348*, pp.10-16.

[3] Buchanan, V.E., Shipway, P.H. and McCartney, D.G., 2007. Microstructure and abrasive wear behaviour of shielded metal arc welding hardfacings used in the sugarcane industry. *Wear*, *263*(1-6), pp.99-110.

[4] Fernandes, F., Polcar, T., Loureiro, A. and Cavaleiro, A., 2015. Effect of the substrate dilution on the room and high temperature tribological behaviour of Ni-based coatings deposited by PTA on grey cast iron. *Surface and Coatings Technology*, *281*, pp.11-19.

[5] Ding, X., Li, X., Huang, H., Matthias, W., Huang, S. and Feng, Q., 2018. Effect of Mo addition on as-cast microstructures and properties of grey cast irons. *Materials Science and Engineering: A*, *718*, pp.483-491.

[6] Pouranvari, M., 2010. On the weldability of grey cast iron using nickel based filler metal. *Materials & Design*, *31*(7), pp.3253-3258.

[7] Cui, C., Guo, Z., Wang, H. and Hu, J., 2007. In situ TiC particles reinforced grey cast iron composite fabricated by laser cladding of Ni–Ti–C system. *Journal of Materials Processing Technology*, *183*(2-3), pp.380-385.

[8] Buchanan, V.E., Shipway, P.H. and McCartney, D.G., 2007. Microstructure and abrasive wear behaviour of shielded metal arc welding hardfacings used in the sugarcane industry. *Wear*, *263*(1-6), pp.99-110.

[9] Qi, X., Jia, Z., Yang, Q. and Yang, Y., 2011. Effects of vanadium additive on structure property and tribological performance of high chromium cast iron hardfacing metal. *Surface and Coatings Technology*, *205*(23-24), pp.5510-5514.

[10] Qu, Y., Xing, J., Zhi, X., Peng, J. and Fu, H., 2008. Effect of cerium on the as-cast microstructure of a hypereutectic high chromium cast iron. *Materials letters*, *62*(17-18), pp.3024-3027.

[11] Zhi, X., Xing, J., Fu, H. and Xiao, B., 2008. Effect of niobium on the as-cast microstructure of hypereutectic high chromium cast iron. *Materials letters*, *62*(6-7), pp.857-860.

[12] Prado, R.V., Uquillas, B., Aguilar, J.Y., Aguilar, Y. and Casanova, F., 2010. Abrasive wear effect of sugarcane juice on sugarcane rolls. *Wear*, *270*(1-2), pp.83-87.

[13] Zhong, M., Liu, W. and Zhang, H., 2006. Corrosion and wear resistance characteristics of NiCr coating by laser alloying with powder feeding on grey iron liner. *Wear*, *260*(11-12), pp.1349-1355.

[14] Womersley, D., 1990. Thermal spraying and powder spray welding processes for the hardfacing of grey cast iron. *Materials & Design*, *11*(3), pp.153-155.

[15] Chatterjee, S. and Pal, T.K., 2003. Wear behaviour of hardfacing deposits on cast iron. *Wear*, *255*(1-6), pp.417-425.

[16] Coronado, J.J., Caicedo, H.F. and Gómez, A.L., 2009. The effects of welding processes on abrasive wear resistance for hardfacing deposits. *Tribology International*, *42*(5), pp.745-749.

[17] Fan, C., Chen, M.C., Chang, C.M. and Wu, W., 2006. Microstructure change caused by (Cr, Fe) 23C6 carbides in high chromium Fe–Cr–C hardfacing alloys. *Surface and Coatings Technology*, *201*(3-4), pp.908-912.

[18] Chung, R.J., Tang, X., Li, D.Y., Hinckley, B. and Dolman, K., 2009. Effects of titanium addition on microstructure and wear resistance of hypereutectic high chromium cast iron Fe–25wt.% Cr–4wt.% C. *Wear*, *267*(1-4), pp.356-361.

[19] Shule, X.I.N.G., Shengfu, Y.U., Yu, D.E.N.G., Minghui, D.A.I. and Lu, Y.U., 2012. Effect of cerium on abrasive wear behaviour of hardfacing alloy. *Journal of Rare Earths*, *30*(1), pp.69-73.

[20] Wiengmoon, A., Pearce, J.T.H. and Chairuangsri, T., 2011. Relationship between microstructure, hardness and corrosion resistance in 20 wt.% Cr, 27 wt.% Cr and 36 wt.% Cr high chromium cast irons. *Materials Chemistry and Physics*, *125*(3), pp.739-748.

[21] Wiengmoon, A., Pearce, J.T.H., Nusen, S. and Chairuangsri, T., 2016. Effects of Si on microstructure and phase transformation at elevated temperatures in ferritic white cast irons. *Materials Characterization*, *120*, pp.159-167.